ÇUKUROVA UNIVERSITY
INSTITUTE OF NATURAL AND APPLIED SCIENCES

MSc THESIS

Aydın İNCEDERE

DETECTION OF EXUDATES FROM DIGITAL FUNDUS IMAGES OF DIABETIC RETINOPATHY PATIENTS

DEPARTMENT OF ELECTRICAL AND ELECTRONICS ENGINEERING

ADANA, 2018

ÇUKUROVA UNIVERSITY
INSTITUTE OF NATURAL AND APPLIED SCIENCES

DETECTION OF EXUDATES FROM DIGITAL FUNDUS IMAGES OF DIABETIC RETINOPATHY PATIENTS

Aydın İNCEDERE

MSc THESIS

DEPARTMENT OF ELECTRICAL AND ELECTRONICS ENGINEERING

We certify that the thesis titled above was reviewed and approved for the award of degree of the Master of Science by the board of jury on 01/02/2018

……	……	……...
Assoc. Prof. Dr. Sami ARICA	Assist. Prof. Dr. Şule ÇOLAK	Assist. Prof. Dr. Ahmet AYDIN
SUPERVISOR	MEMBER	MEMBER

This MSc Thesis is written at the Department of Institute of Natural And Applied Sciences of Çukurova University.
Registration Number:

Prof. Dr. Mustafa GÖK
Director
Institute of Natural and Applied Science

ABSTRACT

MSc THESIS

DETECTION OF EXUDATES FROM DIGITAL FUNDUS IMAGES OF DIABETIC RETINOPATHY PATIENTS

Aydın İNCEDERE

ÇUKUROVA UNIVERSITY
INSTITUTE OF NATURAL AND APPLIED SCIENCES
DEPARTMENT OF ELECTRICAL AND ELECTRONICS ENGINEERING

Supervisor : Assoc. Prof. Dr. Sami ARICA
Year : 2018, Pages 66
Jury : Assoc. Prof. Dr. Sami ARICA
: Assist. Prof. Dr. Şule ÇOLAK
: Assist. Prof. Dr. Ahmet AYDIN

Diabetes is a condition where the body does not produce enough insulin to convert sugar to energy, leading to a build up of sugar in the blood. This leads to a number of problems, including diabetic retinopathy. Diabetic retinopathy is a complication of diabetes that causes damage to the blood vessels of the retina that allowing you to see fine detail. It causes progressive damage to the retina. One of the earliest and most common symptoms of exudate diseases leading to blindness such as diabetic retinopathy and macular degeneration. Some areas of the retina with these conditions must be photocoagulated by laser to stop the progression of the disease and prevelant diseases. Deliminating these areas depends on the delineation of the lesions and anatomical structures of the retina. In this thesis we proposes a simple yet an efficient approach for automatic detection of the exudates of the Diabetic Retinopathy. The detection of exudates of diabetic retinopathy is composed of four main steps: 1. Max filtering of the fudus image converted to grayscale. 2. Fitting a polynomial curve composed of three line segments to the cumalative histogram and specified the second break level as a threhold level 3. Removing optic disk and false exudate regions from the image 4. Finally thresholding the image in the determined regions to get exudates. After exudate detection statistics of exudates have also been computed. The main contribution of this thesis is the automatic threshold level specification approach. The method is verified by an expert and it is seen that the proposed method is promising.

Key Words: Diabetic retinopathy, optic disk, exudate, fundus image, max-filter, image segmentation, image thresholding.

ÖZ

YÜKSEK LİSANS TEZİ

DİYABETİK RETİNOPATİ HASTALARINA AİT SAYISAL GÖZ DİBİ GÖRÜNTÜLERİNDEN EKSUDALARIN TESPİTİ

Aydın İNCEDERE

ÇUKUROVA ÜNİVERSİTESİ
FEN BİLİMLERİ ENSTİTÜSÜ
ELEKTRİK ELEKTRONİK MÜHENDİSLİĞİ ANABİLİM DALI

Danışman : Doç. Dr. Sami ARICA
Yıl : 2018, Sayfa 66
Jüri : Doç. Dr. Sami ARICA
: Yrd. Doç. Dr. Şule ÇOLAK
: Yrd. Doç. Dr. Ahmet AYDIN

Diabet, vücudun, şekeri enerjiye çevirmek için yeterli insülini üretemeyerek kandaki şekerin artmasına yol açma durumudur. Bu durum Diyabetik retinopati gibi bir çok probleme yol açar. Diyabetik retinopati, görmemizi sağlayan retinanın kan damarlarına zarar veren diyabetin komplikasyonudur. Bu retinanın aşamalı olarak zarar görmesine neden olur. Eksüdanın en eski ve yaygın semptomlarından birisi diyabetik retinopati ve macula hasarı gibi körlüğe neden olan rahatsızlıklardır. Retinanın bazı bölgeleri bu durumlarda hastalığın ilerleyişini durdurmak için lazer kullanılarak fotokoagüle edilmelidir. Bu bölgeleri belirlemek lezyonların ve retinanın anatomic yapısına bağlıdır. Bu tez, diyabetik retinopatinin neden olduğu eksüdaların otomatik tespiti için basit ve etkili bir yaklaşım sunmaktadır. Diyabetik Retinopatinin neden olduğu exudaların tespiti dört esas adımdan meydana gelir. 1. Gri dönüşümü yapılmış görüntünün maksimum filtresi. 2. Üç doğru segmentinden oluşan polinom eğrisinin kümülatif histograma uydurulması ve ikinci kırılım seviyesinin eşik değer seviyesi olarak belirlenmesi. 3. Optik disk ve hatalı eksüda bölgelerinin görüntüden kaldırılması. 4. Son olarak eksüdaları elde etmek için belirlenmiş bölgeler içinde görüntünün eşiklenmesi. Eksüdaların tespiti sonrası eksüdaların istatistiği hesaplanmaktadır. Bu tezin ana katkısı otomatik olarak eşik seviyesinin belirlenmesi yaklaşımıdır. Metot uzmanlar tarafından doğrulanmış ve önerilen metodun umut verici olduğu görülmüştür.

Anahtar Kelimeler: Diyabetik retinopati, optik disk, eksüda, fundus görüntüsü, maksimum filtre, görüntü segmentasyonu, görüntü eşikleme.

ACKNOWLEDGEMENTS

I would like to express my deep gratitude to my thesis supervisor Assoc. Prof. Dr. Sami ARICA for his excellent guidance, support and patience. Special thanks to Dr. Burcu Harç KAYA, Dr. Fariba CAFERNEJAD and Maya Eye Hospital for providing the digital color fundus images and evaluating the results of my study. I am also much grateful to my father Faruk İNCEDERE and my wife Fatma İNCEDERE for their spiritual support in the face of difficulties.

CONTENTS **PAGE**

LIST OF FIGURES **PAGE**

LIST OF ABBREVIATIONS

DR	: Diabetic Retinopathy
MAX	: Maximum
NTSC	: National Television System Committee
RGB	: Red Green Blue
R&D	: Research and Development
DPI	: Dots Per Inch
NPDR	: Non-Proliferative Diabetic Retinopathy
HEMs	: Hemorrhages
PDR	: Proliferative Diabetic Retinopathy
MAs	: Microaneurysm
NN	: Neural Network
BLs	: Bright lesions

1. INTRODUCTION

1.1. Diabet

International Diabetes Federation defines the diabet as “Diabetes” is a chronic disease that happens when the pancreas is no longer able to make insulin, or when the body cannot make acceptable use of the insulin it produces. Insulin is a hormone made by the pancreas, that acts like a key to let glucose from the food we eat pass from the blood stream into the cells in the body to produce energy. All carbohydrate foods are broken down into glucose in the blood. Insulin helps glucose get into the cells.

Not being able to produce insulin or use it effectively leads to raised glucose levels in the blood (known as hyperglycaemia). Over the long-term high glucose levels are associated with damage to the body and failure of various organs and tissues.”

1.2. Diabetic Retinopathy

Diabetic retinopathy is a progressive damage of the blood vessels in the retina of patients who have diabetes. Early recognition can arrest or reverse the expansion of the disease and keep from blindness. Diabetic retinopathy first shows itself slowly over the years as background retinopathy, which is the early stage of diabetic retinopathy. At this early stage, tiny blood spots appear on the retina. Increasing retinopathy develops from background retinopathy and is responsible for most of the visual loss in diabetics. In this condition, new blood vessels improve on the surface of the retina. These immature blood vessels tend to burst and bleed into the cavity of the eye. Scar tissue can also form from the ruptured blood vessels and can contract and pull on the retina, causing vision loss. There is two kinds of DR: non-proliferative diabetic retinopathy (NPDR) and proliferative diabetic retinopathy (PDR). The first stage of DR is NPDR and can be defined as mild, moderate or severe. With this situation, the blood vessels’s walls in the retina

become feeble. Very small protrusions protrude from the vessel walls, sometimes leaking or outflow fluid and blood into the retina. Also, sometimes, deposits of cholesterol or other fats from the blood may leak into the retina. NPDR can cause several alterations in the eye, including microaneurysms (MAs), hemorrhages (HEMs) and exudates which are bright lesions (BLs) (as for instance hard and soft exudates). PDR is the more advanced shape of the disease, where smashable new blood vessels form on the surface of the retina over time. These abnormal vessels can bleed or develop scar tissue causing severe loss of vision. PDR may induce more stern vision loss than NPDR because it can have an impact both central and peripheral vision. Because of this reason it is very important to diagnose and treat DR in the non-proliferative stage. One of the methods to diagnose DR is processing of digital fundus images. They are the visual digital images which are the appearance of a patient's retina, the retinal vasculature and the optic disk. Figure 1.1 shows the digital image of normal and diabetic retina. The acquisition of fundus images is easy to perform. Therefore they are adapted for large scale screening purposes. Computer-aided determination and diagnosis of DR with retinal fundus images significantly lessens the burden of the execution of a widely screening of the diabetic patients.

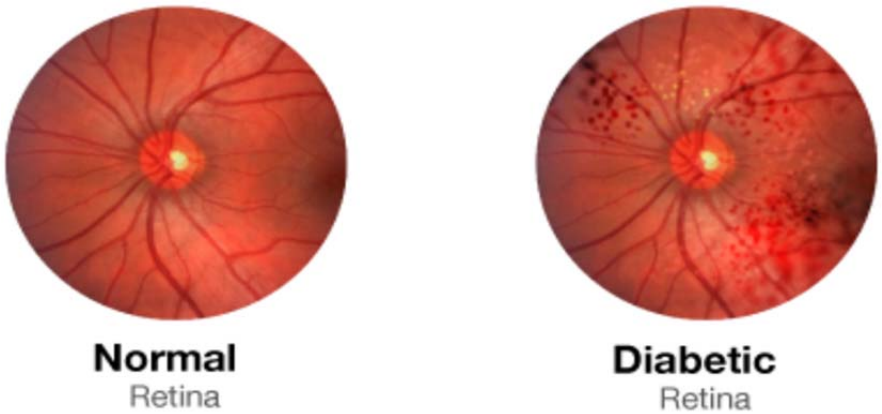

Fig 1.1. The Digital Image of Normal Retina and Diabetic Retina

2. PREVIOUS STUDIES ABOUT THE DETECTION OF DR

Recent years have seen the development of methods for the accurate detection of exudates by considering them individually and in a collective way. These methods, that are combined in a sequential and suitableway, are appropriate for exploring the particular characteristics of the lesions (that by nature are very diverse in shape, size, texture and color). Some novel contextual features are derived and quantified, for each lesion depending on the lesion specific properties. Then the corresponding numerical feature values are used to obtain a binary classification method. Standard performance measures such as sensitivity and specificity are used for its evaluation. We mention here some of these works on automated detection of DR. Non linear diffusion segmentation is used to segment out the exudates by K.Narasimhan et al . The segmentation of exudates using fuzzy c-means clustering algorithm is done by Akara et al. Also, color normalization and local contrast enhancement followed by fuzzy C-means clustering and neural networks were used by Osareh et al. Gardner et al. proposed an automatic detection of diabetic retinopathy using an artificial neural network. The exudates are identified from grey level images by Gardner et al. In a new hybrid classifier as an ensemble of Gaussian mixture model and support vector machine is proposed for exudate detection by M.U.Akram et al. As for mathematical morphology based exudate detection methods, vessels and optic disk are removed first, then mathematical morphology operators are performed to obtain the exudates. Sopharak et al. used a closing operator and reconstruction operators together with thresholding to remove the optic disk and main vessels, then discriminate the exudate pixels according to the local variation due to exudate pixels have high contrast to its surrounding pixels. In Giancardo's method for the diagnosis of diabetic macular edema based on exudate detection is proposed et al. Akita et al. supply a study to identify the skeleton of the blood vessel tree based on line

identifying in fundus images. For identifying the optic disc, they determine the average degree of a window centered on the points of blood vessel intersection inside the optic disc area. Points of degree greater than a threshold were used to approximate calculation of the optic disc area. They also supply the technique of an exudates detection on base of mathematical morphology and subtraction. Less than normal and faint exudates are too difficult to find to be detected as they stated. Also, false negative results were obtained because artifacts from noise in image asset can be defined as lessions which are exudates in that method. Exudates are detected using k-means clustering also, to calculate intensity difference map after median filtering by W.Hsu et al. This study gives a specificity of seventy four percent. Osareh et.al. used k-means clustering algorithm. Following enhancement of contrast and normalization of color in the HIS color space. As being exudates or non-exudates a neural network was then used to classify areas. The calculation complexity of such algorithms makes it unappropriate due to the very long time needed for process. Sopharak et al. applied median filtering operation for noise reduction and contrast-limited adaptive histogram equalization for contrast enhancement in the HIS color space. Then, they used morphological closing reconstruction techniques for the detection of exudates and optic disc. The technique can give distance information between the detected exudates and the macula. But small and faint exudates are too elusive to be detected. Also, incorrect positive exudates were identified in normal fundus image. As a further method, artifacts from noise in image acquisition can be identified as exudates in this technique. D.Youssef et.al. propose a robust method for the identifying of blood vessels based on edge detection and morphological image processing to make better detection of exudates. This method would help greatly rise the correct value of previous detection of exudates in digital fundus images. The contours of exudates could be detected after removing the blood vessels from the image. The exudates region’ edges were become larger and used as a marker image. The full

extent of exudates could be obtained selectively by morphological reconstruction. This method could be completely automated by its principle to the whole image to extract the whole blood vessel tree, hemorrhage and optic disc. It can also be semi automated by applying the algorithm to certain regions of the image where exudates present. This would increase the sensitivity and specificity of exudates detection. Most of the hopeful methods of lessions which are exudates determintion are based on edge detection algorithms which non-selectively detect edges of all objects. Thus, the defying is to extract the edges of exudates among all other edges. Retinal fundus image analysis currently attracts lots of attention from both computer science field and ophthalmology. Its aim is to develop computational tools which will assist quantification and visualization of the anatomical structures and lesions. It includes vessels analysis, optic disk analysis, macular analysis, micro-aneurysms detection and exudate detection. In this paper, we don't use special technique to remove optic disc and vessels. We review the existing works on exudate detection since our work mainly focus on bright lesions which are exudates. Much work has been performed for exudate detection based on variety of techniques. Most techniques refered previous worked on dilated pupils in which the exudates and other retinal features are obviously visible. Based on experimental work reported in previous work, smart quality images with larger fields are necessary. The retinal images must be obvious enough to show retinal detail.

3. MATERIALS AND METHODS

Digital Fundus image processing currently develop from computer science field. There are lots of materials and methods in digital fundus image processing. In the following we mention our materials and methods.

3.1. Materials

In this thesis we tested our algorithm on forty diabetic retinopathy fundus images which have similar characteristics. These fundus images were taken from 20 females and 20 males who have exudates as a cause of Diabetic Retinopathy. They were collected from the Ankara Maya Göz Hospital. All the results of our study have been approved by ophthalmologists Dr. Burcu Harç Kaya and Dr. Fariba Cafernejad from the Ankara Maya Göz Hospital, Turkey. All images were acquired using Topcon TRC-50EX fundus camera at 35 degree field of view. The camera were subjectively equalized for calibration, luminance and contrast before recording. The bit depth of images is 24-bit color and scaled to 1840x1224 pixels. The resolution of images are 96 dpi in horizontal and vertical dimensions. In some cases, due to the retinal surface difference, the images will have different appearance. Although some changes have been in visual features, the appearances of the fundus images were natural and bare. The method of the study was realized by using Matlab R2015b.

3.2. Methods

The method presented here can be schematically described by means of the block diagram of figure 3.2.

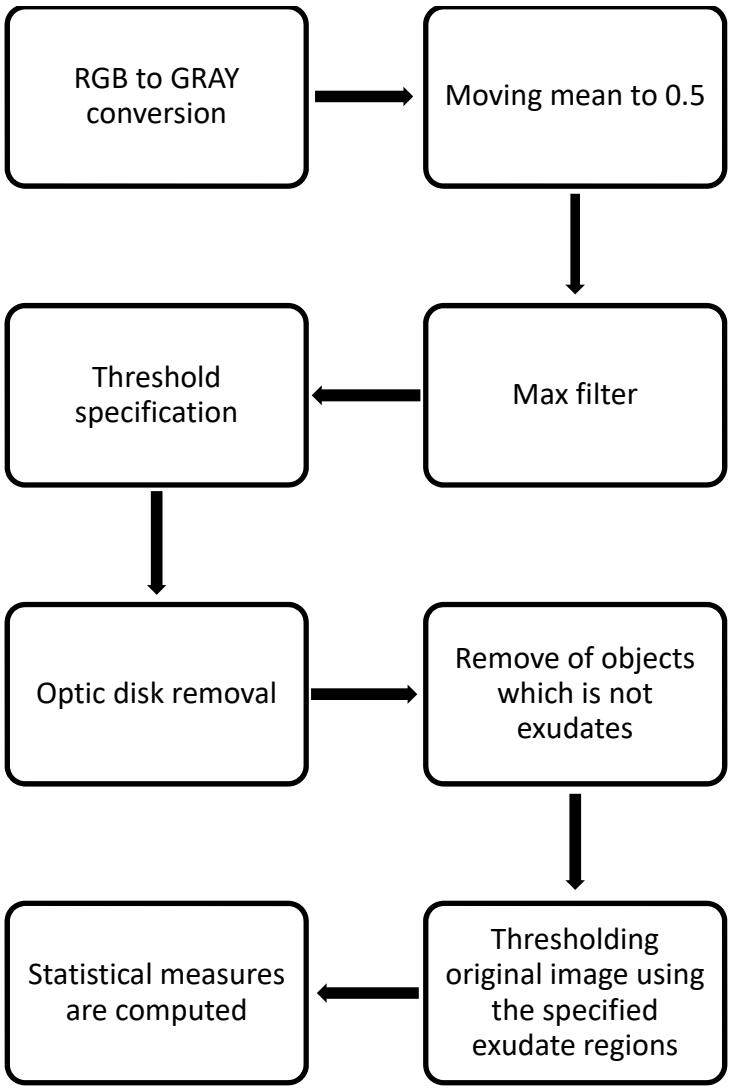

Fig 3.2. Block diagram of proposed method

In this part, the methods used are summarized; the definitions and specifications of the methods are recalled. The block diagram of the approach is provide in figure 3.2. In the following, we describe the steps of the algorithm.

1. RGB image is converted to gray image. Y channel of NTSC color space is computed from RGB image (equation 3.1). And scaled to [0,1] range. A sample fundus image converted to gray scale is given in figure 3.3.

$$Y = 0.2989\,R + 0.5870\;G + 0.1140\,B \tag{3.1}$$

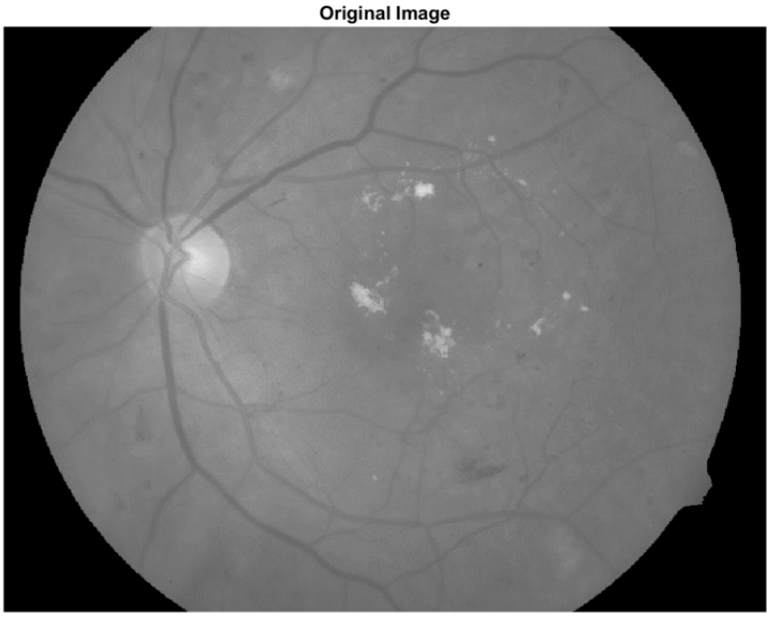

Fig 3.3. A sample fundus image with exudates converted to gray scale diagram of proposed method.

2. The field of view (pupil) of the fundus image is extracted. The region is specified by thresholding the image. The pixels with brightness higher than 0.1 is considered field of view. If more than two connected components distinct regions are obtained by thresholding the biggest connected component (region) is regarded field of view. Next the mean brightness (value) in the field of view Y is moved to 0.5. The following linear transformation(equation 3.2) is employed.

$$\mathrm{I} = \frac{-1}{2\,m-2}\,Y + \frac{2\,m-1}{2\,m-2} \tag{3.2}$$

3. Using 21x21 size overlapping window (20 samples overlap in horizontal and vertical directions) max filter (equation 3.3) is applied.

3.2.1. Order Statistics Filters

Spatial Filters that are based on ordering the pixel values that make up the neighbourhood operated on by the filter.

Useful spatial filters include

- Median filter
- Max and min filter
- Midpoint filter
- Alpha trimmed mean filter

3.2.1.1. Max Filter

Max filter is a non linear order statistic filter. Figure 3.3 shows the max filter operator. Whereas the minimum filter replaces the central pixel with the darkest one in the running window, the maximum filter replaces it with the lightest one. To find the brightest points in an image, finds the maximum value in the area encompassed by the filter. Max filter is good for pepper noise. Reduces the pepper noise as a result of the max operation. In this study, exudates are bright areas according to their surrounding. By using max filter brightness areas which are exudates are enhanced and darkness areas are suppressed.

$$y(m,n) = max_{i,j}\, I(n+i, m+j), i, j = -11 \dots, 11. \quad (3.3)$$

For the image in figure 3.3 the max filter output is as follows.

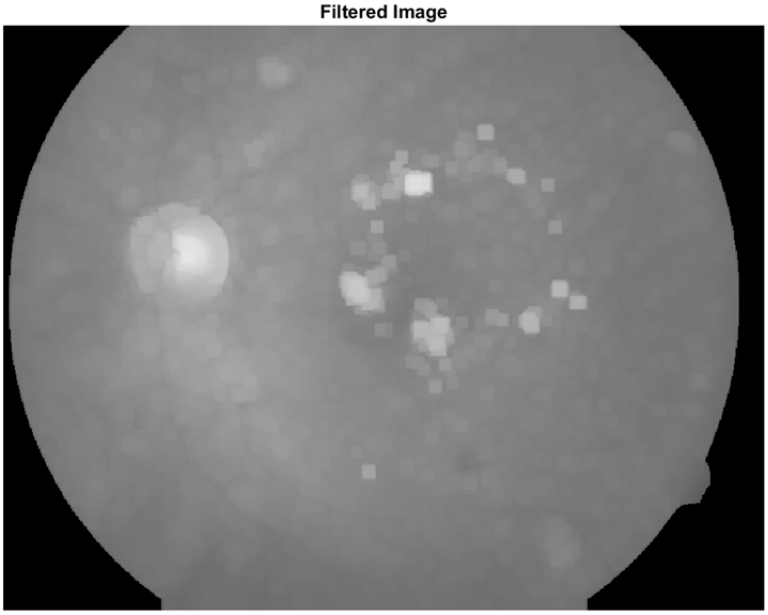

Fig 3.4. Max. filter output

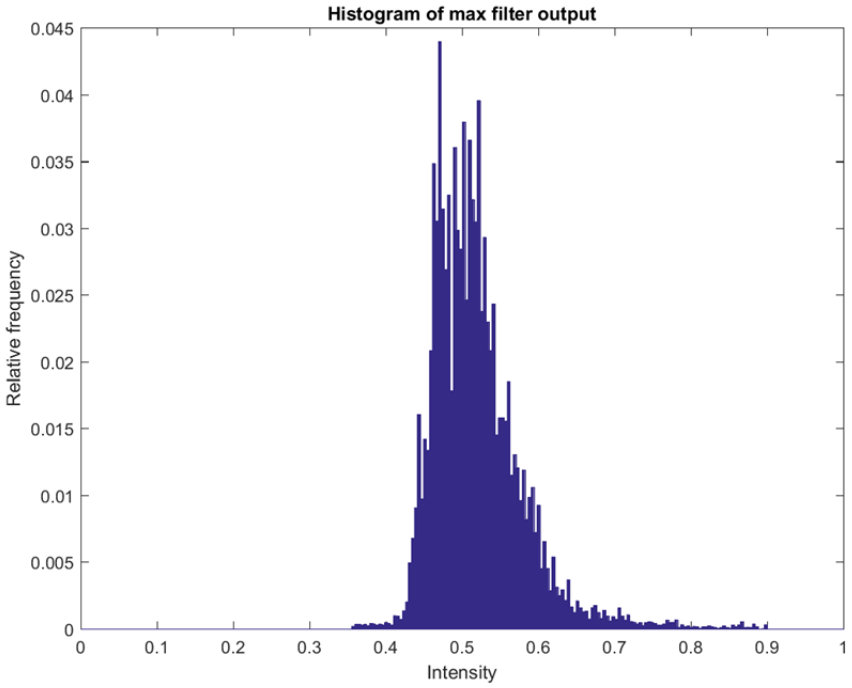

Fig 3.5. Histogram of the max-filter output

4. A polygonal line consists of three line segments is fitted to cumulative histogram of image y. The cumulative histogram is given by

$$c(k) = \frac{number\ of\ pixels \leq k}{total\ number\ of\ pixels}\ ,\ k = (0,1,\dots,255)/255 \tag{3.4}$$

A polygonal curve denoted by $\mathrm{g}(k) = \mathrm{P}(a_1, a_2, a_3, a_4; k)$ is fitted to the cumulative histogram. Here, a_n, a_{n+1} are initial and end point of n-th line segment respectively. The unknown points are optimized such that mean square of error

$e(k) = c(k) - g(k)$ is minimum:

$$\min_{a_1,a_2,a_3,a_4} \sum_{k=0}^{1} \big(c(k) - g(k)\big)^2, \quad \text{subject to} \quad g(1) - g(0) = 1 \tag{3.5}$$

The polygonal curve and cumulative histogram are shown in figure 3.10.
The threshold is then selected as

$$\mathrm{THR} = x(3) - 0.1\,\big(x(3) - x(2)\big) \tag{3.6}$$

where $x(n)$ is the abcissa of the point a_n. The term $0.1\,\big(x(3) - x(2)\big)$ is substructed from $x(3)$ because the the break is not sharp in the cumulative histogram.

3.2.2. Image Thresholding

Image thresholding is a simple, yet effective, way of partitioning an image into a foreground and background. This image analysis technique is a type of image segmentation that isolates objects by converting grayscale images into

binary images. Image thresholding is most effective in images with high levels of contrast.

Common image thresholding algorithms include histogram and multi-level thresholding. Thresholding consists of segmenting an image into two regions: a particle region and a background region. In its most simple form, this process works by setting to white all pixels that belong to a gray-level interval, called the threshold interval, and setting all other pixels in the image to black. The resulting image is referred to as a binary image. For color images, three thresholds must be specified, one for each color component. The threshold can be chosen manually or by using automated techniques. Manual threshold selection is normally done by trial and error, using a histogram as a guide. Automated thresholding techniques select a threshold which optimizes a specified characteristic of the resulting images. These techniques include clustering, entropy, metric, moments, and interclass variance. Clustering is unique in that it is a multi-class thresholding method. In other words, instead of producing only binary images it can specify multiple threshold levels which result in images with three or more gray-level values.

An example for binary original image resulting from the thresholding operation is shown here:

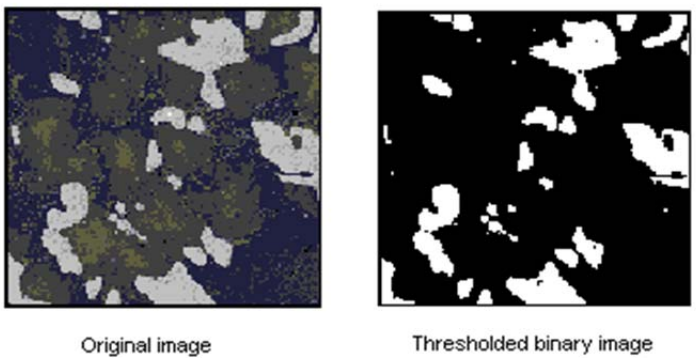

Fig 3.6. An example of image thresholding

3.2.3. Image Histogram

An image histogram is a type of histogram that acts as a graphical representation of the tonal distribution in a digital image. It plots the number of pixels for each tonal value. By looking at the histogram for a specific image a viewer will be able to judge the entire tonal distribution at a glance. Image histograms are present on many modern digital cameras. Photographers can use them as an aid to show the distribution of tones captured, and whether image detail has been lost to blown-out highlights or blacked-out shadows. This is less useful when using a raw image format, as the dynamic range of the displayed image may only be an approximation to that in the raw file. The horizontal axis of the graph represents the tonal variations, while the vertical axis represents the number of pixels in that particular tone. The left side of the horizontal axis represents the black and dark areas, the middle represents medium grey and the right hand side represents light and pure white areas. The vertical axis represents the size of the area that is captured in each one of these zones. Thus, the histogram for a very dark image will have the majority of its data points on the left side and center of the graph. Conversely, the histogram for a very bright image with few dark areas and/or shadows will have most of its data points on the right side and center of the graph.

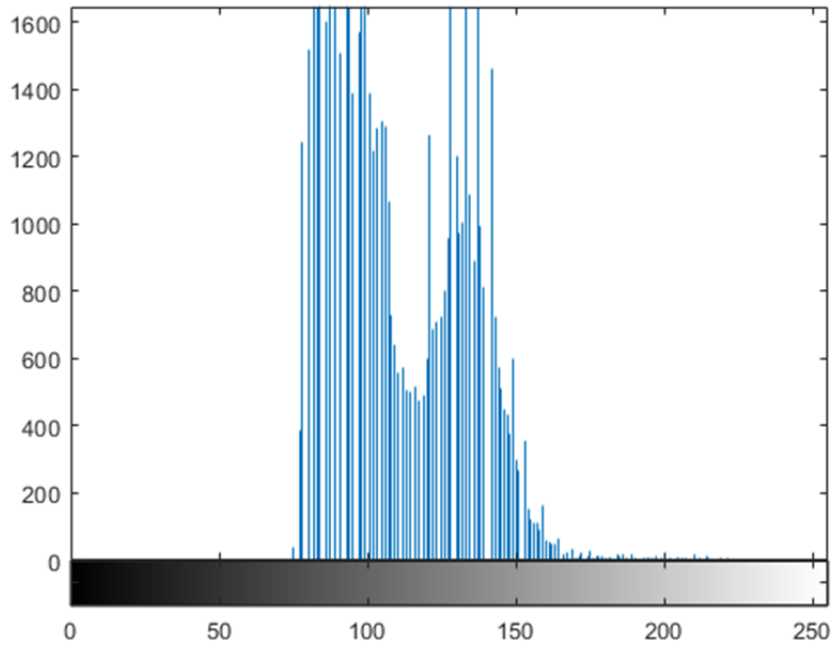

Fig 3.7. An example of image histogram

3.2.3.1. Cumulative Histogram

The cumulative histogram is a histogram in which the vertical axis gives not just the counts for a single bin, but rather gives the counts for that bin plus all bins for smaller values of the response variable. A cumulative histogram is a mapping that counts the cumulative number of observations in all of the bins up to the specified bin. That is, the cumulative histogram Mi of a histogram mj is defined as:

$$Mi = \sum_{j=1}^{i} mj \tag{3.7}$$

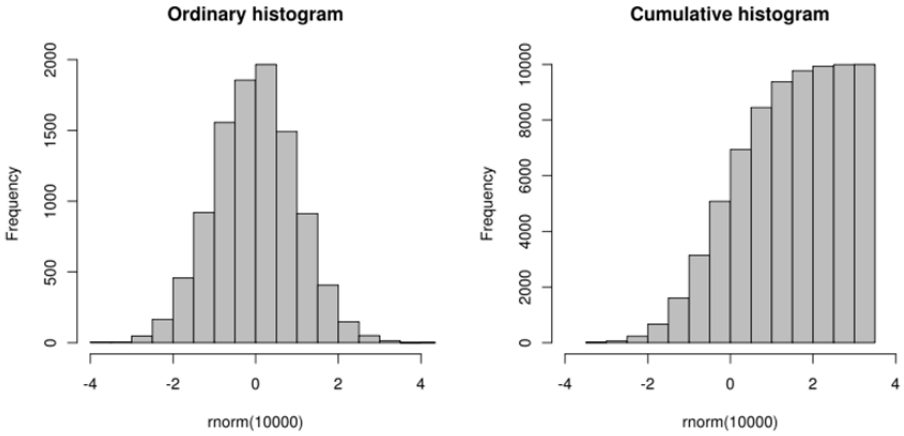

Fig 3.8. An example of Ordinary and Cumulative Histogram

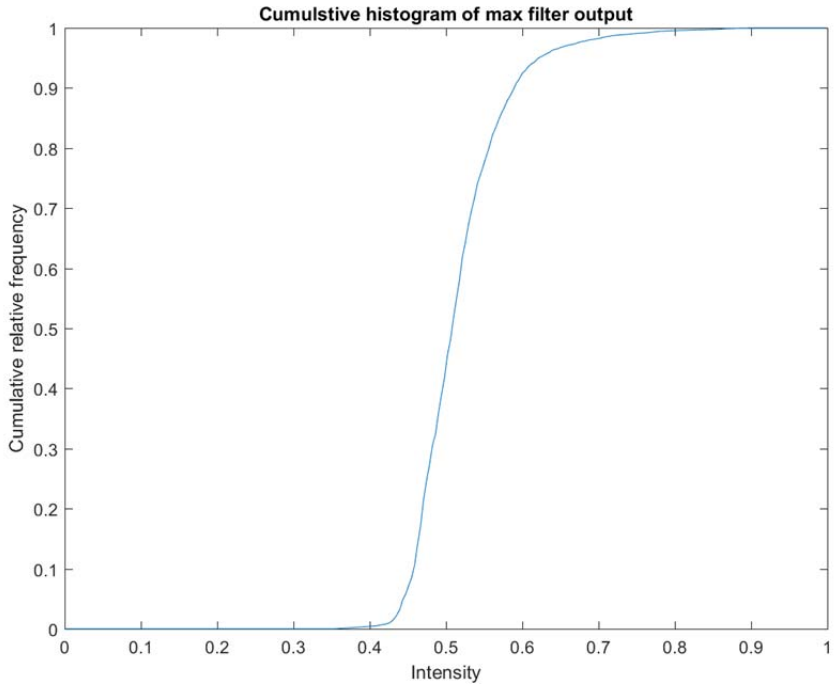

Fig 3.9. Cumulative histogram of Max.filter

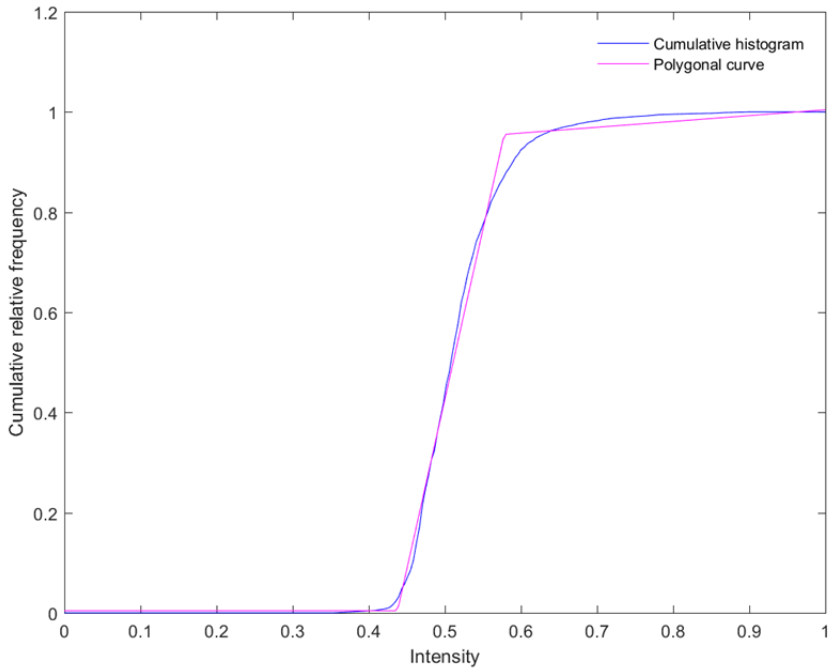

Fig 3.10. Cumulative histogram and Polygonal curve

5. After thresholding connected components are obtained and the component with highest area is considered optic disk (together with reflected light about the disk) and removed. Similarly the objects with major axis length greater than quarter of major axis length of the field of view are regarded as scattering of light from the border of the pupil.

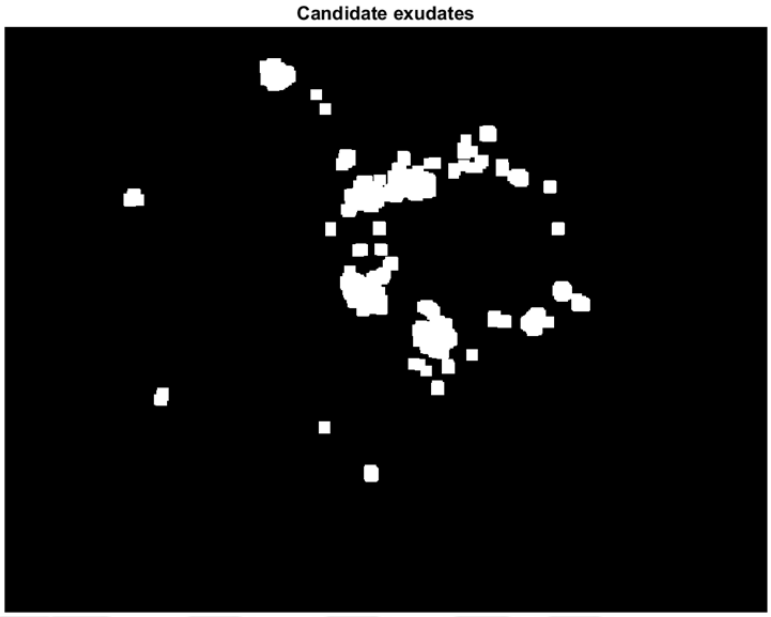

Fig 3.11. Candidate exudates

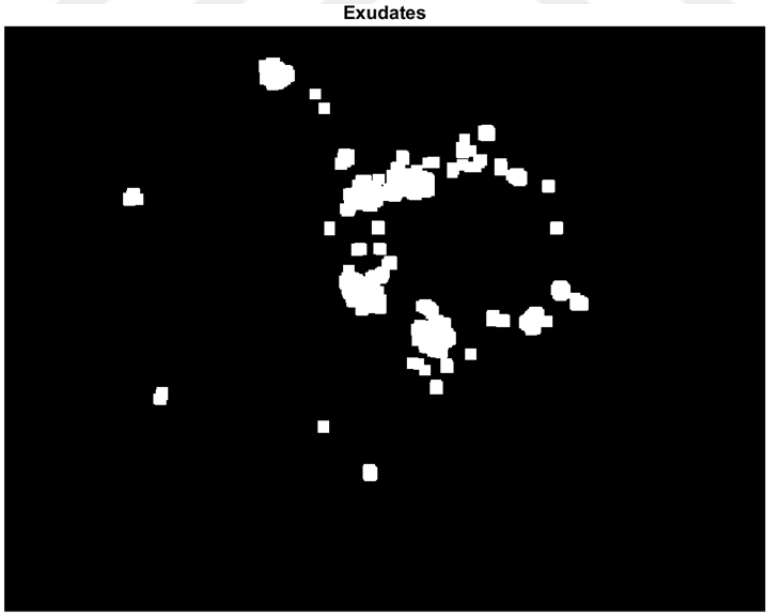

Fig 3.12. Exudates

6. To obtain final segmentation, the pixels of the image I in the regions obtained are thresholded with the threshold obtained in step 4. With this threshold we detect the location of exudates which are shown in figure 3.14.

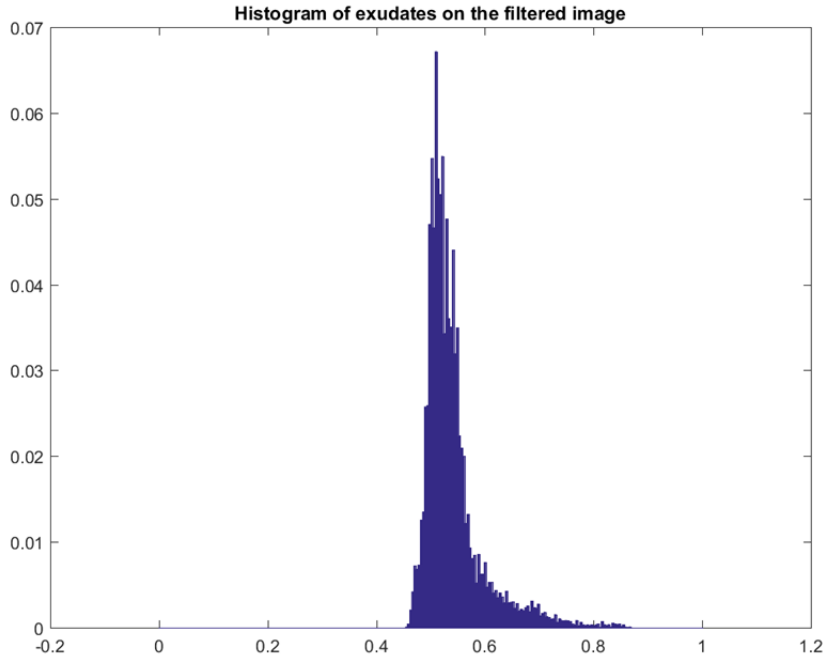

Fig 3.13. Histogram of exudates on the filtered im

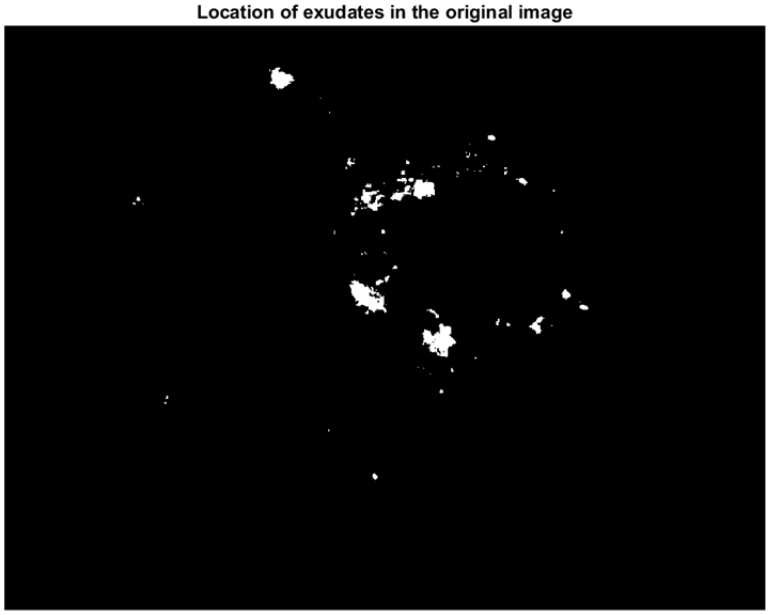

Fig 3.14. Location of exudates in the original image

At early stage of our study we tried the Otsu method but we didn't get good result for our data. The image is considered to have three parts; backround, eye and exudates. Therefore two threshold is computed for segmenting image into three regions by using Otsu method and the highest threshold is used for extracting excudates. Thresholding of output of max-filter by employing Otsu method are tested on three different fundus images. In figures 3.16, 3.18, 3.20 the results for Otsu and our method are shown for comparision. From the figures it is deduced that the most of the excudates are covered with our method while Othsu method miss some of the excudates or inaccurately specifies some regions as exudates.

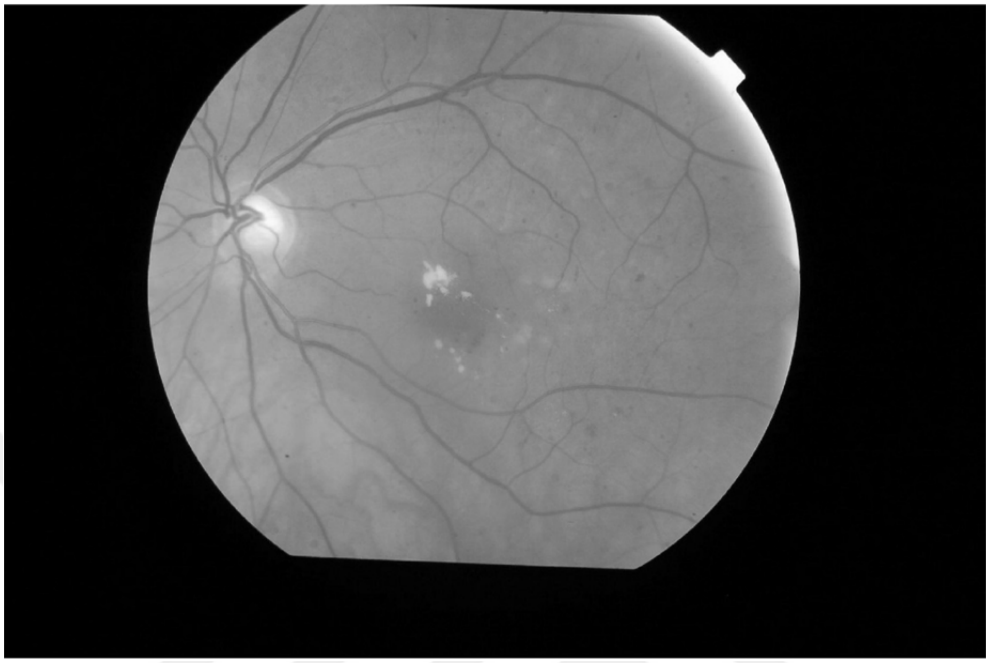

Fig 3.15. Original Image 1 for Otsu analyzing

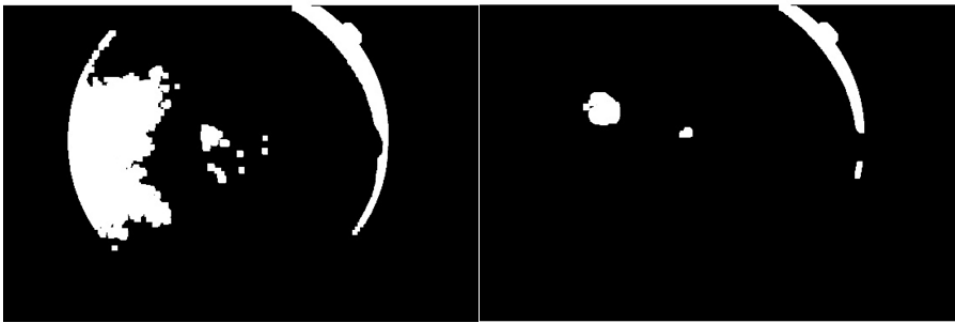

Fig 3.16. The results for Our Method (left) and Otsu Method (right) of Image 1

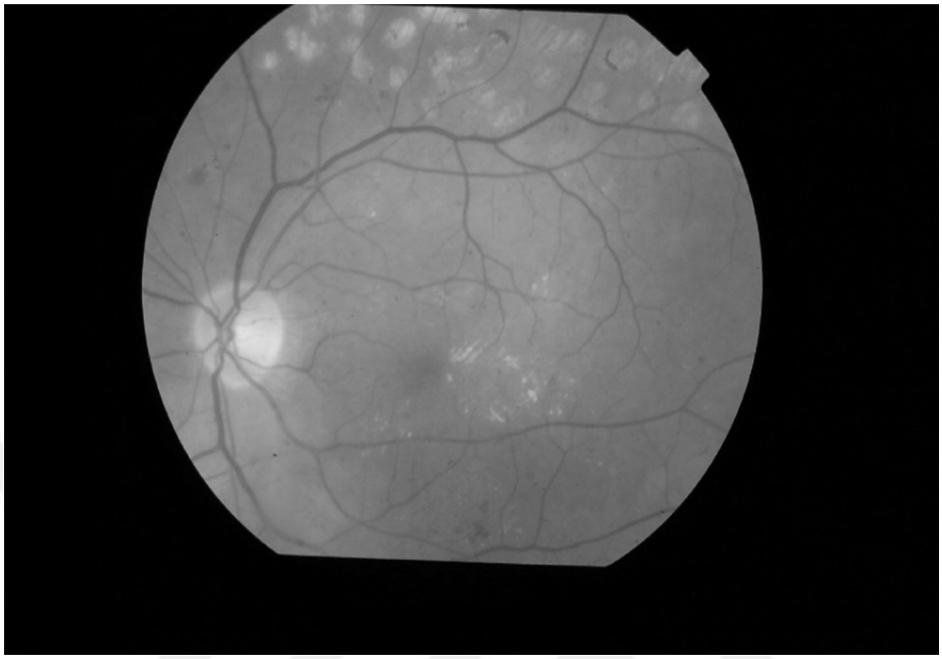

Fig 3.17. Original Image 2 for Otsu analyzing

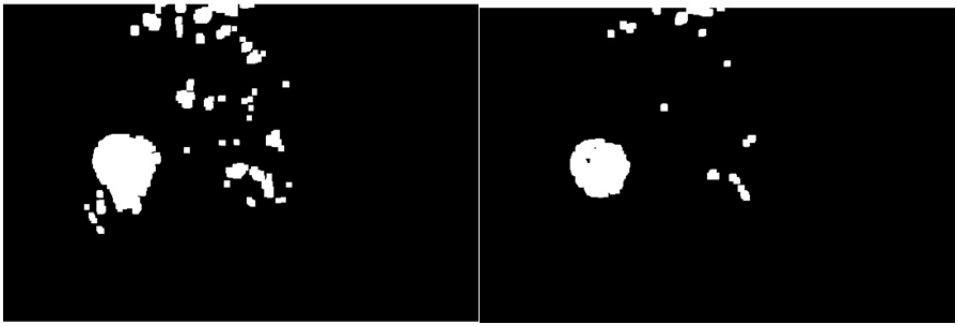

Fig 3.18. The results for Our Method (left) and Otsu Method (right) of Image 2

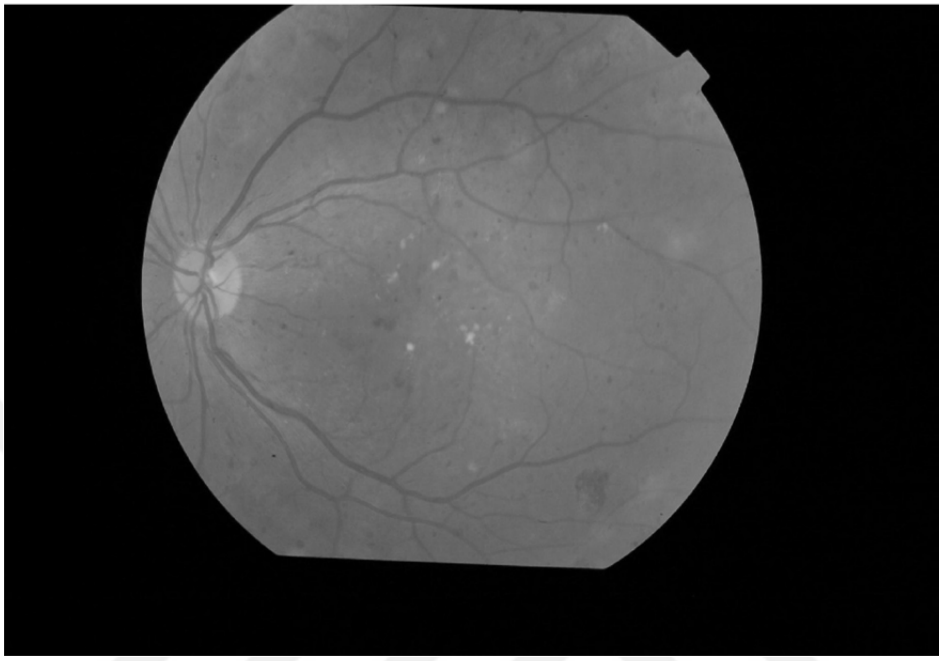

Fig 3.19. Original Image 3 for Otsu analyzing

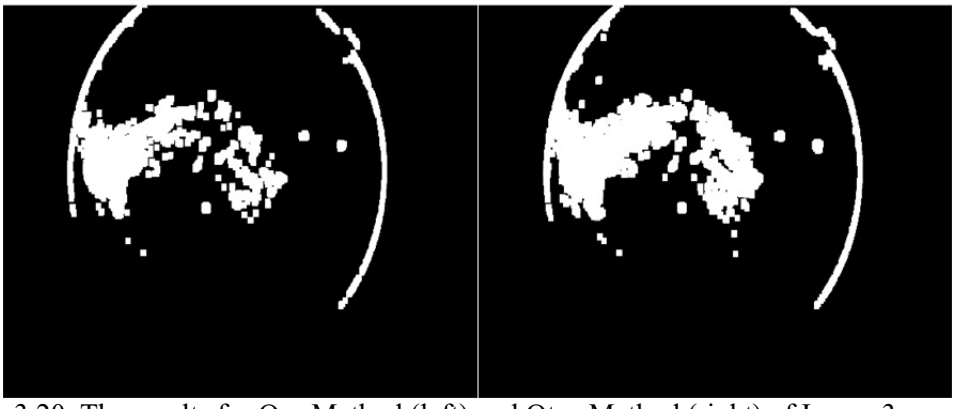

Fig 3.20. The results for Our Method (left) and Otsu Method (right) of Image 3

7. Finally, we compute two statistical measures from the segmented image. Percentage of total exudates in the field of view = total area of exudates / pupil area.

   Percentage of the biggest exudate = the highest exudate area / total area of exudates.

4. RESULTS

In this thesis, we propose a simple yet an efficient method on the fundus images with dispersed exudates. We classified our results as good, normal and bad. The results were controlled by two ophthalmologists and they gave 0 point for bad results, 0.5 point for normal result and 1 point for good result. As a result they gave 20 points in total for our good results, 7.5 point in total for normal results and 0 point in total for bad results. They gave totally 27.5 point over 40 point. The average point is 0.6875. When we reference our 40 digital fundus images, according to two ophthalmologists the success rate of this study is 50% good results, 37.5% normal results, 12.5% bad results.

A-) *Good-segmented image:*

In figure 4.1, a good segmentation of the image is reported. The method removes optic disk and finds exudates. Figure 4.2 shows the location of exudates which is the sample for a good segmented image. In our 40 digital fundus images we got 20 good results thus we got 20 point. Our success rate is 50% for good segmented image class.

Fig 4.1. Original image for a good segmentation

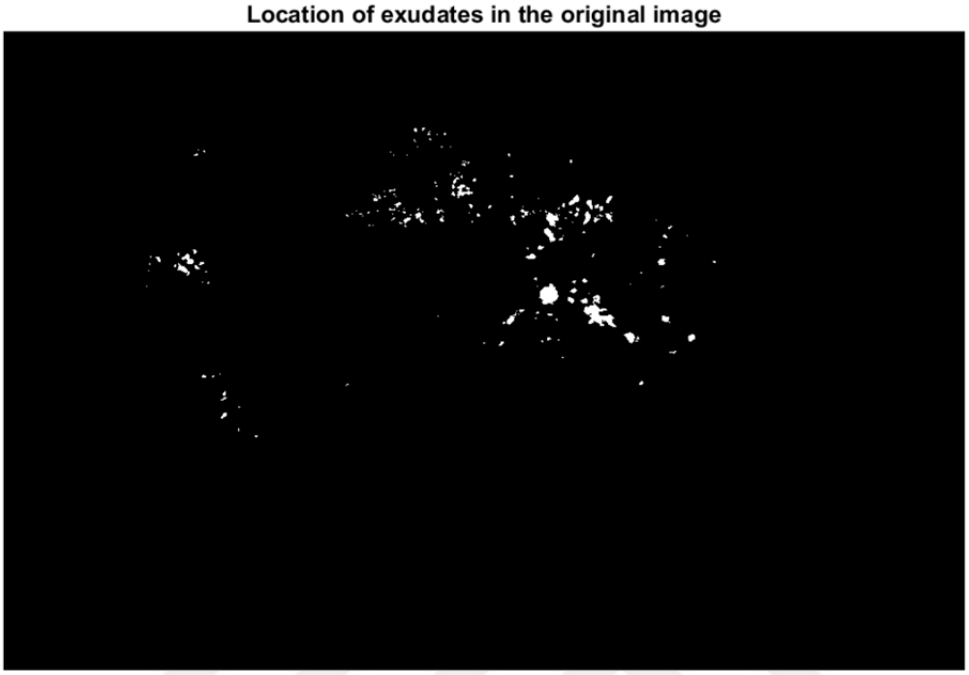

Fig 4.2. Location of exudates for a good segmentation

B-) *Fair-segmented image:*

In 15 images of our 40 images, there is reflection at the boundaries of the fundus image due to camera light. This reflection effect success of exudate detection because these light reflections may be regarded exudates by the algorithm. The proposed algorithm also eliminates these reflected areas. We eliminate these areas by using major axis length. Due to the shape for all exudates close to circular shape we got reference for major axis length value of these exudate shapes. If a major axis length value match for an exudate it is not eliminated but if it is not matched, this is a reflection area and it is eliminated.The fundus image and its detected exudates given in figure 4.4 and 4.6 is a demonstration of this capacity. In our 40 digital fundus images we got 15 normal

results thus we got 7.5 point. Our success rate is 37.5% for normal segmented image class.

Fig 4.3. Original image for a normal segmentation in sample 1

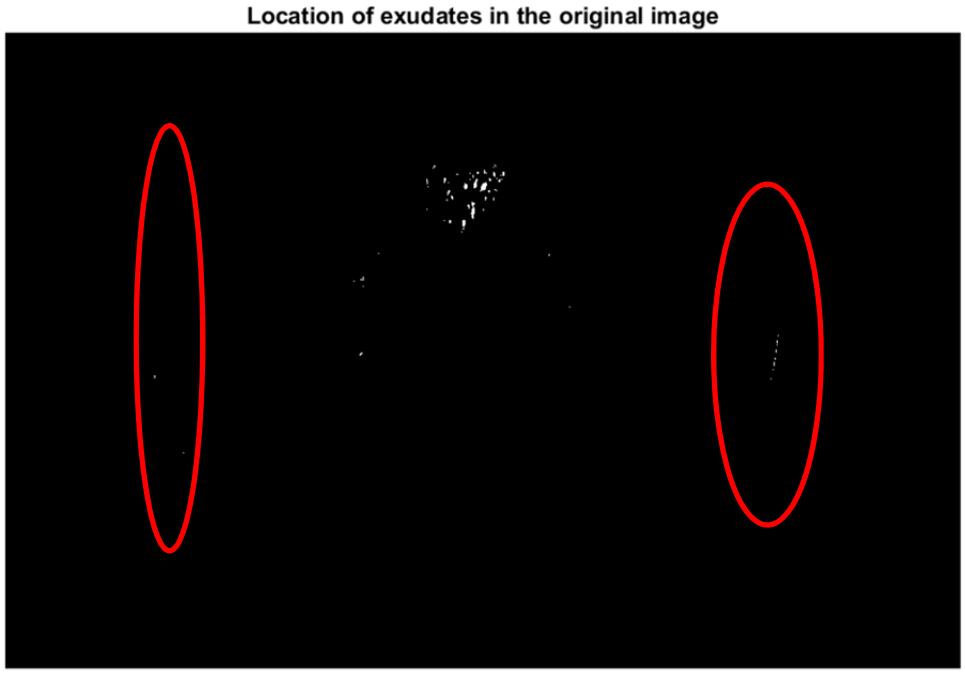

Fig 4.4. Location of exudates for a normal segmentation in sample 1

Fig 4.5. Original image for a normal segmentation in sample 2

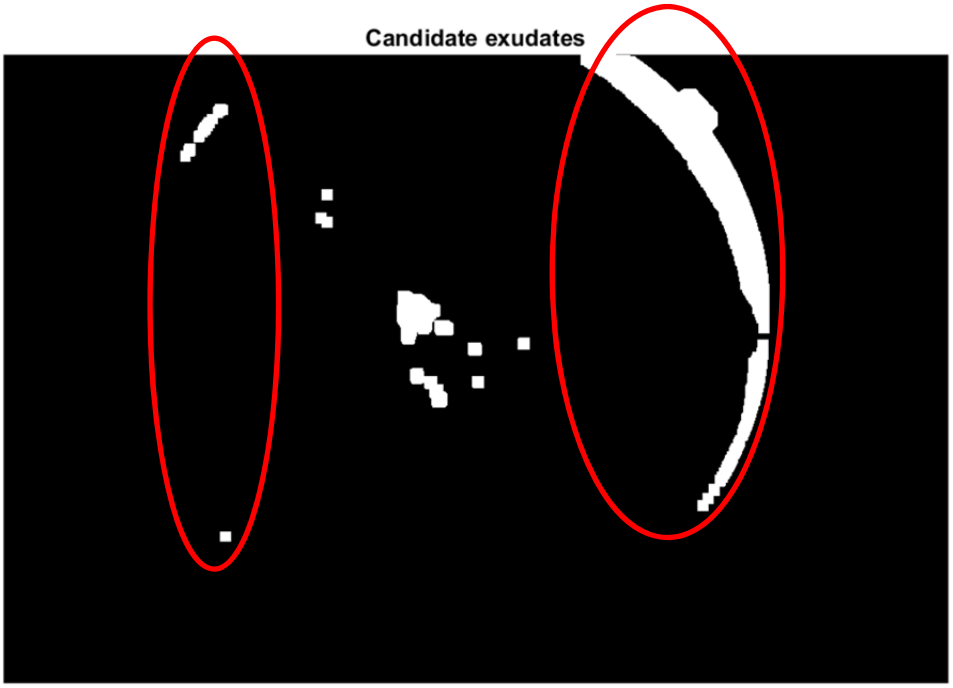

Fig 4.6. Candidate Exudates for a normal segmentation in sample 2

C-) *Bad-segmented image:*

The algorithm fails when exudates are not dispersed, the grouping resulted by max filter is higher than the optic disk and gives bad results when the exudates are bigger than the optic disk diameter or major axis length of the reflected light at boundaries. In our 5 images of 40 fundus images we got bad result. So the the ratio of bad segmented image is 12.5%. Figure 4.7 shows an example of this situation. When we apply our method to this image, we don't get only exudates, we also get optic disc in figure 4.8.

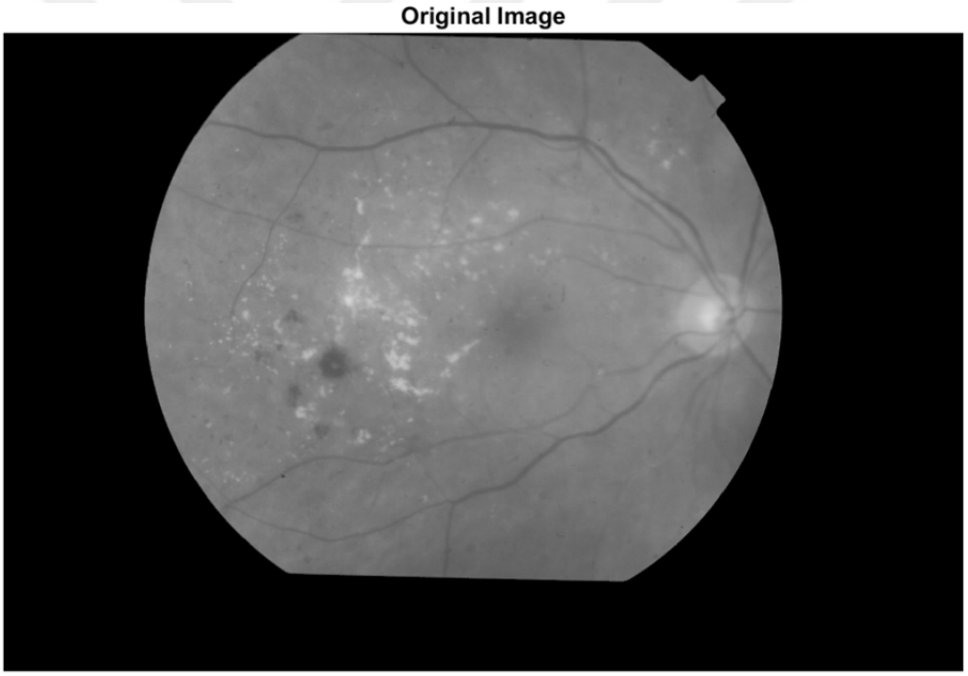

Fig 4.7. Original image for a bad segmentation

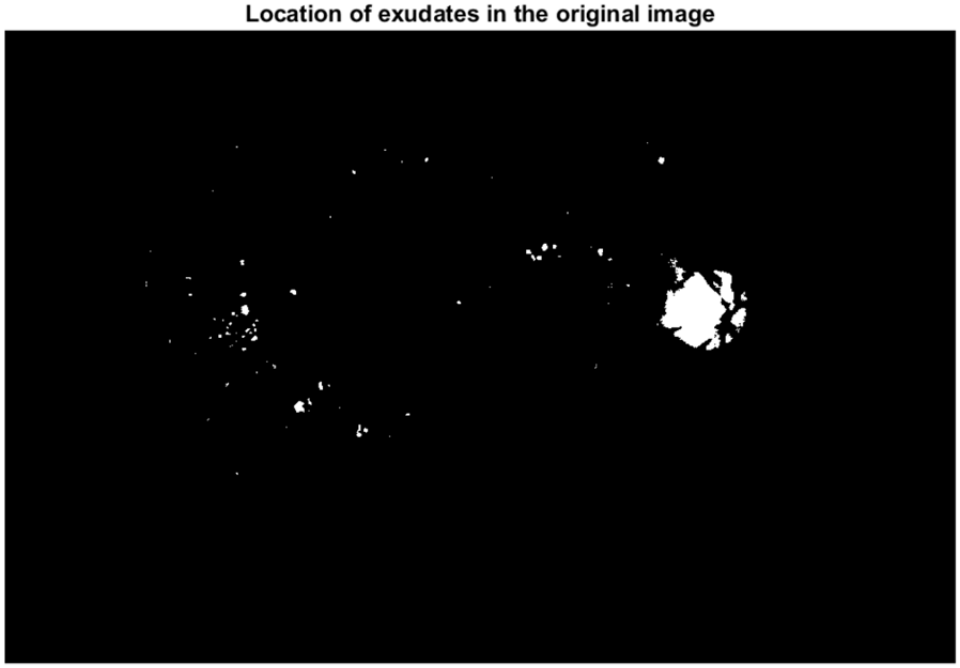

Fig 4.8. Location of exudates for a bad segmentation

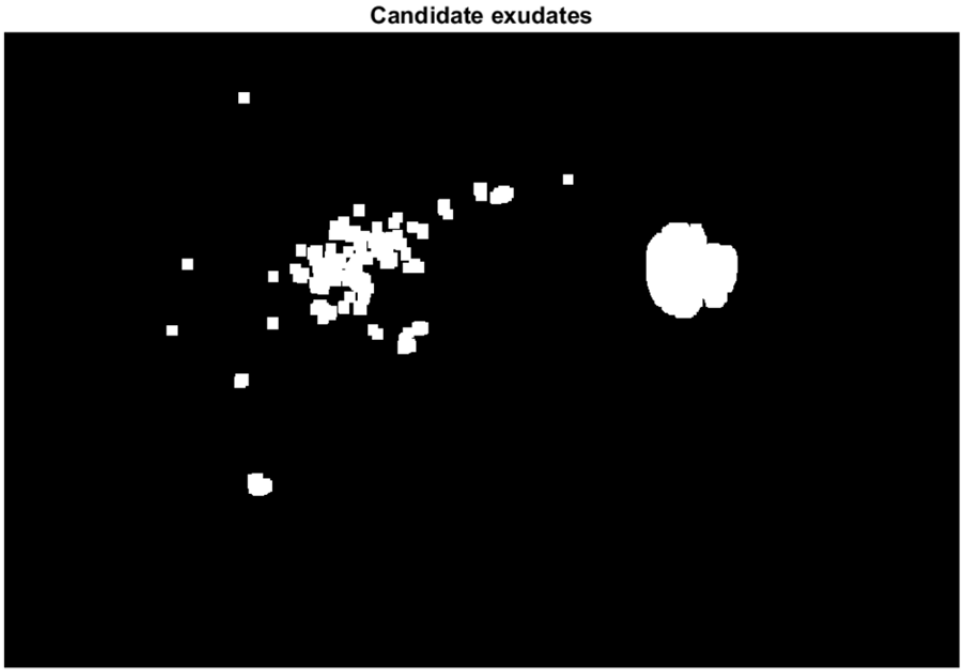

Fig 4.9. Candidate exudates for a bad segmentation

In our study after exudate detection, statistics of exudates have also been computed. We compute two statistical measure. One is percentage of total exudates in the field of view and the other one is percentage of the biggest exudate. These statistical measures are important for observing the progression of disease also analyzing the size and location of exudates.

5. CONCLUSION

With this thesis, diabetic retinopathy exudates were detected. Our algorithm generally perform well but when the exudates (their groping by the algorithm) are bigger than the optic disk, it cannot remove it because we do not use a disk removal technique for just removing optic disk. Simply a segmented region, after max filtering, with the biggest area is removed. At early stage of our study we tried the Otsu method but we didn't get good result for our data. In the future we will also apply special technique for removing optic disk. It is certainly usefull to detect detection of optic disk before the algorithm is applied for specifying exudates. The Hough Transform can also be used to detect optic disk.

The algorithm can also be modified to detect micro-aneurysms by using negative of the gray image. By this way we will classify exudates and micro-aneurysms. In addition, detection of the lesions at earlier stages is still an open problem.

We tested the method on several color fundus images to assess the performance of our approach. We conclude that the presented method can assist ophthalmologists to specify exudates and help to overcome the problem of contrast, incorrect illumination and noise while examining the fundus images. Additionally it may also support specialist for monitoring the progression of disease and aid for a better treatment plan.

REFERENCES

AKITA, K., KUGA, H. A., (1982) Computer method of understanding ocular fundus images, Pattern Recognition, *IEEE*, 15 (6) 431–443.

AKRAM, M.U., TARIQ, A., KHAN, S.A., JAVED, M.Y. (2014) Automatic detection of exudates and macula for grading of diabetic macular edema, *BIOMED*, 141-152.

CHEN, Y., WEMURI, B.C., WANG, L. (2000) Image Denoising and Segmentation via Nonlinear Diffusion. *ELSEVIE*R, 131-149.

FIGUEIREDO, I.N., KUMAR, S., OLIEIRA, C.M., RAMOS, J.D., ENGQUIST, B.(2015) Automated Lesion Detectors in Reinal Fundus Images. *ELSEVIER*, 47-65

GARDNER, G.G., KEATING, D., WILLIAMSON, T.H., ELLIOTT, A.T. (1996). Automatic detection of diabetic retinopathy using an artificial neural network: a screening tool. *British journal of Ophthalmology*, 940-944

GIANCARDO, L., MERIDEUAEU, F., KARNOWSKI, T.P, Y. Li, S. GARG, TOBIN, K.W., CHAUM,E. (2012) Exudate-based diabetic macular edema detection in fundus images using publicly available datasets, MED. IMAGE ANAL, 16 (1) 216–226.

HSU, W., P.M.D.S. Pallawala, Lee, M.L., Eong, G.A., The role of domain knowledge in the detection of retinal hard exudates, (2001) *IEEE Conference on Computer Vision and Pattern Recognition*

JIMENEZ, S., ALEMANY, P., FONDON, I., FONCUBIERTA, A., ACHA, B., & SERRANO, C. (2010) Automatic Detection of Vessels in Color Fundus Images, *ELSEVIER*, 103-109.

KUMARI, C.J., MARUTHI, R. (2012) Detection of Hard Exudates in Color Fundus Images of the Human Retina, *ELSEVIER*, 297-302.

KUMAR, P., DEVARAJ, D., & MANISHA. (2013) Automatic exudates detection for the diagnosis of the diabetic retinopathy. *International Journal of innovative research and studies,* 2, 658-669.

LIU, Q., ZOU, B. CHEN, J., KE, W., YUE, K., CHEN, Z., ZHAO, G. (2017) Alocation to segmentation strategy for automatic exudate segmentation in color retinal fundus images. *ELSEVIER*, 78-86

MITTAL, D., KUMARI, K. (2015) Automated detection and segmentation of Drusen in Retinal Fundus Images. *ELSEVIER*, 82-95

NARASIMHAN, K., NEHA, V.C. & VJAYAREKHA, K. (2012). A review of automated diabetic retinopathy diagnosis from fundus image. *Journel of theoretical and applied information technology,* 39, 225-238.

OSAREH, A., MIRMEHDI, M., THOMAS, B., MARKHAM, R., (2003) Automated identification of diabetic retinal exudates in digital color images, *British Journal of Ophthalmology* (87) 1220–1223.

SHAH, J., (1991) Segmentation by nonlinear diffusion, *IEEE*, pp 202-207

SOPHARAK, A., UYYANONVARA, B., BARMAN, S., WILLIAMSON, T.H. (2008) Automatic detection of diabetic retinopathy exudates from non-dilated retinal images using mathematical morphology methods. *Comput. Med. Imaging Graph*, 720-727.

SOPHARAK, A., UYYANONVARA, B., & BARMAN, S. (2009).” Automatic Exudate Detection from Non-dilated Diabetic Retinopathy Retinal Images Using Fuzzy C-means Clustering” Sensors , 9, 2148- 2161.

T.P .KARNOWSKI, T.P., AYKAC, D., GIANCARDO, L., LI, Y., NICHOLS, T., TOBIN, K.W., & CHAUM, E. (2011) Automatic Detection of Retina Disease :Robustness to image quality and localization of anatomy structure . *IEEE transactions on biomedical engineering*, 5959-5964.

WALTER, T., MASSIN, P., ERGINAY, A., ORDONEZ, R., JEULIN, C., KLEIN, J.C. (2007) Automatic Detection of Microaneurysms in color fundus images. *ELSEVIER*, 555-566.

WU, B., ZHU, W., SHI, F., ZHU, S., CHEN, X. (2017) Automatic Detection of Microaneurysms in Retinal Fundus Imges. *ELSEVIER*, 106-112.

YOUSSEF, D., SOLOUMA, N., (2012). Accurate detection of blood vessels improves the detection of exudates in color fundus images. *ELSEVIER, (*39), 225-238.

ZHU, C., ZOU, B., ZHAO, R., CUI, J., DUAN, X., CHEN, Z., LIANG, Y. (2017) Retinal Vessel Segmentation in Color Fundus Images using Extreme Learning Machine. *ELSEVIER*, 68-77

BIOGRAPHY

Aydın İNCEDERE was born in HATAY, Turkey in 1984. He received his B.S. degree in Electronics and Communication Engineering Department from Yıldız Technical University in 2009. After completion his B.S. education, he enrolled MSc education in Electrical and Electronics Engineering Department in Cukurova University in 2012. He has been working as a Specialist System Engineer in the Aselsan since June, 2016. Network Engineer in Turkish Telecom between 2012-2016. R&D Engineer in Nortel Netas between 2009-2012. His research areas are Signal and Image Processing and Computer Networks.

APPENDICES

Appendix 1: Matlab Codes Used for Implimenting the Algorithm

```
% Collective result


%
% Obtain list of the image files in the current folder.
p ='C:\Users\aincedere\Desktop\tez_kod_110917\40_FUNDUS\';

dlist = strcat(p,'*.jpg');
s = dir(dlist);
files = char( s.name );

L = size(files, 1);
C = cell(1, L);
K = cell(1, L);
THR = zeros(1, L);
P = zeros(1, L);
E = zeros(1, L);
for n = 1:L
    imname = strcat(p, files(n, :));
    img = imread(imname);
    [C{n}, K{n}, THR(n), P(n), E(n)] = enheudates(img, n);
end
```

```
% Enhance Exudates


function  [C, K, THR, P, E] = enheudates(x, k)

close all

if nargin == 1,
    ck = '';
else
    ck = strcat('FI', num2str(k));
end

x = double(x);

if ndims(x) == 3,
    I =  0.2989*x(:, :, 1) + 0.5870*x(:, :, 2) + 0.1140*x(:,
:, 3);
    % Y channel of NTSC color space
    % I =  0.212671*x(:, :, 1) + 0.715160*x(:, :, 2) +
0.072169*x(:, :, 3);
    % Y channel of XYZ color space
else
I = x;
end

% y = I/255;
% y = hsteqbr(I/255); %equalize hisogram if necessary

% m = meanbr(y);
% y = lintrns(y, m);
y = modifymean(I/255, 0.5);

[N, M] = size(y);

% K = 32;
% Q = 1/K;
% yq = round(y/Q);
% yq = yq / (K - 1);

figone = figure(1);
imshow(y, [0.0 1.0]);
title('Original Image');
figname = strcat(ck, 'FIG1');
print(figone, figname,'-dpng')

% Window size
```

```
%W = 11;
W = 21;

% Number of overlapping samples
%D = 10;
D = 20;

V = floor((N - W)/(W - D) + 1);
H = floor((M - W)/(W - D) + 1);


J = zeros((V - 1)*(W - D) + W, (H - 1)*(W - D ) + W);


for v = 0:V-1
    for h = 0:H-1
        % block = yq(v*(W - D) + 1:v*(W - D) + W, h*(W - D) +
1:h*(W - D) + W);
        block = y(v*(W - D) + 1:v*(W - D) + W, h*(W - D) +
1:h*(W - D) + W);
        % s = sort(block(:), 'descend');
        s = unique(block(:));
        J(v*(W - D) + 1:v*(W - D) + W, h*(W - D) + 1:h*(W -
D) + W) = max(s);
    end
end

figtwo = figure(2); imshow(J, [0.0 1.0]);
title('Filtered Image');
figname = strcat(ck, 'FIG2');
print(figtwo,figname,'-dpng')


IM = zeros(N, M, 1, 2);
IM(:,:,1,1) = y;
[N1, M1] = size(J);
tmp = zeros(N, M);
tmp(1:N1, 1:M1) = J;
IM(:,:,1,2) = tmp;
figure(3); montage(IM,'Size', [1 2],'DisplayRange', [0 1]);
% iptsetpref('ImshowBorder','tight')

bns = (0:255)/255;
hst = hist(J(:), bns);
hst(1:16) = 0;
phst = hst / sum(sum(hst));
figfour = figure(4);
```

```
bar(bns, phst, 1);
xlim([0 1])
xlabel('Intensity')
ylabel('Relative frequency')
title('Histogram of max filter output')
figname = strcat(ck, 'FIG4');
print(figfour,figname,'-dpng')


chst = cumsum(phst);
figfive = figure(5);
plot(bns, chst);
xlim([0 1])
xlabel('Intensity')
ylabel('Cumulative relative frequency')
title('Cumulstive histogram of max filter output')
figname = strcat(ck, 'FIG5');
print(figfive,figname,'-dpng')



fun = @(x, xdata) mystpfn(x, xdata);
lb = [0, 0, 0, 0, 0];
ub = [1, 1, 1, 1, 1];

x0 = [0.1, 0.15, 0.2, 0.75, 0.1];
xdata = bns;
ydata = chst;
x = lsqcurvefit(fun, x0, xdata, ydata, lb, ub);

u = mystpfn(x, xdata);

figsix = figure(6);
plot(bns, chst, 'b', xdata, u, 'm');
legend('Cumulative histogram','Polygonal curve')
legend('boxoff')
xlabel('Intensity')
ylabel('Cumulative relative frequency')
figname = strcat(ck, 'FIG6');
print(figsix,figname,'-dpng')

THR = x(4) - (x(4) - x(3))*0.1;

%

BW = J > THR;
```

```
% Optic disk is removed
[LBL, NUM] = bwlabel(BW);

SZ = zeros(NUM, 1);
for num = 1:NUM
    SZ(num) = sum(double(BW(LBL == num)));
end

[~, p] = max(SZ);

BW(LBL == p) = 0;
LBL(LBL == p) = 0;

figseven = figure(7);
imshow(BW, [0 1])
title('Candidate exudates')
figname = strcat(ck, 'FIG7');
print(figseven,figname,'-dpng')


% Normal tissiue and lession seperation
labels = setdiff(1:NUM, p);

LB = zeros(size(LBL));
for num = 1:NUM - 1
    LB(LBL == labels(num)) = num;
end

stats = regionprops(fov(y),
'MajorAxisLength','MinorAxisLength');
A = stats.MajorAxisLength / 10;

MN = zeros(NUM - 1, 7);
% edges = (0:256)/256;
% edges = [bns - 1/2/255, 1 + 1/2/255];
% edges = union(bns - 1/2/255, bns + 1/2/255);
% edges = - 1/2/255:1/255:1 + 1/2/255;

delta = 1/255;
[~, edgs, bns] = meanbr(y, delta);
for num = 1:NUM - 1
    sqn = y(LB == num);
    [avg, pk, ent, skw, krt] = compfeat(sqn, edgs, bns);
    stats = regionprops(LB == num,
'MajorAxisLength','MinorAxisLength');
    a = stats.MajorAxisLength / A;
    b = stats.MinorAxisLength / A;
```

```
    % MN(num, :) = [mean(y(LBL == num)), max(y(LBL == num))];
    MN(num, :) = [avg, pk, ent, skw, krt, a, b];
end

u = MN(:, 6) > 2.5;
pa = find(u);

if not(isempty(pa)),
for p = pa;
BW(LB == p) = 0;
LB(LB == p) = 0;
end


labels = setdiff(NUM - 1, p);
NUMM = length(labels);

LBB = zeros(size(LB));
for num = 1:NUMM
    LBB(LB == labels(num)) = num;
end

MN = MN(not(u), :);

else
    LBB = LB;

end

c = 2;
distance = 'cosine'; % 1 - u*v / norm(u) / norm(v)
% distance = 'mahalanobis'; % sqrt( (u - v)' * (1/S) * (u -
v) )


% k-means clustering
[t, cent] = kmeans(MN, c, 'Distance', distance);


% If the Distance Between Centers are Significant Choose One
Cluster
D = pdist(cent, distance); % distance between rows
% if D < 0.01
if D < 2
B = BW;
else
```

```
[~, m] = max(cent(:, 2)); % Choose cluster where its norm of
center is the highest.

% Choose cluster where its norm of center is the highest.
K = sum(t == m);
k = find(t == m);

B = zeros(size(y));
% L = zeros(size(LBL));
for c = 1:K
    B(LBB == k(c)) = 1;
%    L(LBL == k(c)) = c;
end

end

figeight = figure(8);
imshow(B, [0 1]);
title('Exudates')
figname = strcat(ck, 'FIG8');
print(figeight,figname,'-dpng')

lst = y(logical(B));
bns = (0:255)/255;
h = hist(lst, bns);
h = h / sum(h);
fignine = figure(9);
bar(bns, h, 1)
title('Histogram of exudates on the filtered image')
figname = strcat(ck, 'FIG9');
print(fignine,figname,'-dpng')

ynew = zeros(size(y));
ynew(logical(B)) =  y(logical(B));
C = ynew > THR;

figten = figure(10);
imshow(C, [0 1])
title('Location of exudates in the original image')
figname = strcat(ck, 'FIG10');
print(figten,figname,'-dpng')

lst = y(logical(B));
bns = (0:255)/255;
h = hist(lst, bns);
h = h / sum(h);
figeleven = figure(11);
```

```
bar(bns, h, 1)
title('Histogram of exudates')
figname = strcat(ck, 'FIG11');
print(figeleven,figname,'-dpng')


% Statistical measures

[LBL, NUM] = bwlabel(C);


SZ = zeros(NUM, 1);
for num = 1:NUM
    SZ(num) = sum(double(C(LBL == num)));
end

% [mx, p] = max(SZ);
mx = max(SZ);


P = mx / sum(sum(double(C))) * 100; % Percentage of the
biggest lession

% TH = graythresh(y);
TH = 0.1;
K = y > TH;
figtwelve = figure(12);
imshow(K, [0 1])
title('Fiel of view (pupil)')
figname = strcat(ck, 'FIG12');
print(figtwelve,figname,'-dpng')


E = sum(sum(double(C))) / sum(sum(double(K)))  * 100; %
Percentage of lessions in whole eye
```

```
% Compfeat

function [avg, pk, ent, skw, krt] = compfeat(sqn, edgs, bns)
h = histcounts(sqn, edgs);

thr = 0.2*max(h);
k = h > thr;
p = zeros(size(h));
p(k) = h(k) / sum(h(k));

avg = sum(p .* bns);

[~, k] = max(p);
pk = bns(k);

skw = skewness(p); % d = zeros(1, L). d(1) = 1; K =
skewnes(d, 0);
K = 16;
skw = skw / K; % this is to keep skewness in the range [-1
1].

krt = kurtosis(p);
krt = 1/krt; % This is to map the range [1, Inf] to [0, 1].

ent = - sum(log2(p(ne(p, 0))) .* p(ne(p, 0)));
R = 8; % R = log2(L). % L is the maximum possible number of
bins
ent = ent / R; % this keeps entropy in the range [0 1].
```

```
% fov.m

function y = fov(x, thr)

% field of view
% pupil
% x in [0 1]

if nargin == 1,
thr = 0.1;
end

y = x > thr;

% the 8-connected object
[L, N] = bwlabel(y) ;
% only the biggest region is retained
if N > 1,
stats = regionprops(L,'Area');
% array of structs
vals = [stats.Area];
[~, p] = max(vals);
y = L == p;
end

end
```

```
% lintrns.m

function y = lintrns(x, m)

y = zeros(size(x));

k = x < m;
y(k) = 0.5/m*x(k);

k = x >= m;

y(k) = 0.5/(1 - m)*(x(k) - m) + 0.5;
```

```
% meanbr.m

function [m, edgs, bns] = meanbr(x, delta)


if nargin == 1,
 delta = 1/255;
end

bw = fov(x);
m = mean(x(bw));
m = round(m/delta)*delta;

edgs = m - delta/2: delta: 1 + delta/2;
bns = m : delta: 1;
```

```
% modifymean.m

function y = modifymean(x, m)

bw = fov(x);

mu = mean(x(bw));

y = zeros(size(x));

alpha = (m - 1)/(mu - 1);
mprime = 1 - alpha;

y(bw) = alpha*x(bw) + mprime;

end


% alpha*mu + mprime = m
% alpha + mprime =< m. mprime = 1 - alpha.
% alpha*mu + (1 - alpha) = m
% alpha*(mu - 1) = m - 1;
% alpha = (m - 1)/(mu - 1)
```

```
% mystpfn.m


function y = mystpfn(x, xdata)

% Slopes: x(1) x(2)
% Break points: x(3) x(4)
% Initial : x(5)
% y(1) - y(0) = 1

% x  = [0.1, 0.2, 0.2, 0.7, 0.1];
% xdata = linspace(0, 1, 1001);

A = x(1)*x(3) + x(2)*(1 - x(4));
B = x(4) - x(3) ;
alpha = (1 - A)/B;

if x(4) < x(3)
y = repmat(1.25, size(xdata));
else
k = xdata < x(3);
y(k) = x(1)*xdata(k) + x(5);


k = and(xdata >= x(3), xdata < x(4));
y(k) = x(1)*x(3) + x(5) + alpha*(xdata(k) - x(3));


k = xdata >= x(4);
y(k) = x(1)*x(3) + x(5) + alpha*(x(4) - x(3)) +
x(2)*(xdata(k) - x(4));
end


end


%
% x(1)*x + x(5)
% alpha*(x - x(3)) + x(1)*x(3) + x(5)
% x(2)*(x - x(4)) + alpha*(x(4) - x(3)) + x(1)*x(3) + x(5)
%

% x(3) * [x(5) + x(1)*x(3) + x(5)]/2 + ...
% [x(4) - x(3)]*[x(1)*x(3) + x(5) + alpha*(x(4) - x(3)) +
x(1)*x(3) + x(5)]/2
```

```
% [1 - x(4)]*[x(2)*(1  - x(4)) + alpha*(x(4) - x(3)) +
x(1)*x(3) + x(5)
%  + alpha*(x(4) - x(3)) + x(1)*x(3) + x(5)]/2
%

% x(3) * ( x(5) + x(1)*x(3) + x(5) )/2 = ( 2*x(3)*x(5) +
x(1)*x(3)*x(3) ) /
% 2
% ( x(4) - x(3) ) * ( x(1)*x(3) + x(5) + alpha*(x(4) - x(3))
+ x(1)*x(3) + x(5)
% )/2 = ( 2*x(1)*x(3)*x(4)  + 2*x(4)*x(5) - 2*x(1)*x(3)*x(3)
- 2*x(3)*x(5)  )/2 +
% alpha*(x(4) - x(3)) *(x(4) - x(3)) / 2
% (1 - x(4))*(x(2)*(1  - x(4)) + alpha*(x(4) - x(3)) +
x(1)*x(3) + x(5)
%  + alpha*(x(4) - x(3)) + x(1)*x(3) + x(5)])2 = ( x(2)  -
x(2)*x(4) +
%  2*x(1)*x(3)  + 2*x(5)  - x(4)*x(2) + x(4)*x(2)*x(4)  +
2*(1 -
%  x(4))*alpha*(x(4) - x(3)) ) / 2
%

%  2*x(3)*x(5) + x(1)*x(3)*x(3)
%
% 2*x(1)*x(3)*x(4)  + 2*x(4)*x(5) - 2*x(1)*x(3)*x(3)  -
2*x(3)*x(5)  +
% alpha*(x(4) - x(3)) *(x(4) - x(3))
%
%  x(2)  - x(2)*x(4) +  2*x(1)*x(3)  + 2*x(5)  - x(4)*x(2) +
x(4)*x(2)*x(4)  + 2*(1 -
%  x(4))*alpha*(x(4) - x(3))
%

%
%
% 2*x(1)*x(3)*x(4)  + 2*x(4)*x(5) - x(1)*x(3)*x(3)  +
% alpha*(x(4) - x(3)) *(x(4) - x(3))
%
%  x(2)  - x(2)*x(4) +  2*x(1)*x(3)  + 2*x(5)  - x(4)*x(2) +
x(4)*x(2)*x(4)  + 2*(1 -
%  x(4))*alpha*(x(4) - x(3))
```

Appendix 2: A copy of conference paper produced from the thesis study.

This paper was presented in 2017 21th National Biomedical Engineering Meeting (BIYOMUT 2017). The conference was held in Acıbadem Mehmet Ali Aydınlar University, İstanbul, Turkey, between the dates of November 24-26, 2017.

Detection of Exudates from Digital Fundus Images of Diabetic Retinopathy Patients

Diyabetik Retinopati Hastalarına Ait Sayısal Göz Dibi Görüntülerinden Eksüdaların Tespiti

Aydın İncedere[1], Sami Arıca[2]

1. Electrical and Electronics Engineering, ÇUKUROVA University
aydincedere@hotmail.com

2. Electrical and Electronics Engineering, ÇUKUROVA University
arica@cu.edu.tr

Abstract

Diabetes is a condition where the body does not produce enough insulin to convert sugar to energy, leading to a build up of sugar in the blood. This leads to a number of problems, including diabetic retinopathy. Diabetic retinopathy is a complication of diabetes that causes damage to the blood vessels of the retina that allowing you to see fine detail. It causes progressive damage to the retina. This paper proposes a simple yet an efficient approach for automatic detection of the exudates of the Diabetic Retinopathy. The detection of exudates of diabetic retinopathy is composed of eight steps: 1. RGB to gray conversion. 2. Moving mean to 0.5 3. Max Filter 4. Threshold specification 5. Optic disk removal 6. Remove of objects which is not exudates 7. Thresholding original image using the specified exudate regions 8. Computing statistical measures.

Özetçe

Diabet, vücudun, şekeri enerjiye çevirmek için yeterli insülini üretemeyerek kandaki şekerin artmasına yol açma durumudur. Bu durum Diyabetik retinopati gibi bir çok probleme yol açar. Diyabetik retinopati, görmemizi sağlayan retinanın kan damarlarınıa zarar veren diyabetin komplikasyonudur. Bu bildiri, diyabetik retinopatinin neden olduğu eksüdaların otomatik tespiti için basit ve etkili bir yaklaşım sınmaktadır. Eksudaların otomatik tespiti altı adımdan oluşmaktadır. 1. RGB gri dönüşümü. 2. Ortalama değerin 0.5 'e getirilmesi 3. Max Filtrelemele. 4. Eşikleme tanımlama 5. Optic diskin kaldırılması 6. Eksüda dışındaki objelerin kaldırılması 7. Belirlenmiş eksüda bölgelerini kullanarak orjinal görüntüyü eşikleme. 8. İstatistiksel ölçümlerin hesaplanması.

1. INTRODUCTION

Diabetic retinopathy is a progressive damage of the blood vessels in the retina of patients who have diabetes. Early recognition can arrest or reverse the expansion of the disease and keep from blindness. Diabetic retinopathy first shows itself slowly over the years as background retinopathy, which is the early stage of diabetic retinopathy. At this early stage, tiny blood spots appear on the retina. Increasing retinopathy develops from background retinopathy and is responsible for most of the visual loss in diabetics. In this condition, new blood vessels improve on the surface of the retina. These immature blood vessels tend to burst and bleed into the cavity of the eye. Scar tissue can also form from the ruptured blood vessels and can contract and pull on the retina, causing vision loss. One of the methods to diagnose DR is processing of digital fundus images. They are the visual digital images which are the appearance of a patient's retina, the retinal vasculature and the optic disk. The acquisition of fundus images is easy to perform. Therefore they are adapted for large scale screening purposes. Computer-aided detection and diagnosis of DR with

retinal fundus images significantly lessens the burden of the implementation of a large scale screening of the diabetic patients. Recent years have seen the development of methods for the accurate detection of exudates by considering them individually and in a collective way. We mention here some of these works on automated detection of DR. Non linear diffusion segmentation is used to segment out the exudates by K.Narasimhan et al [1]. The segmentation of exudates using fuzzy c-means clustering algorithm is done by Akara et al [2].

Also, color normalization and local contrast enhancement followed by fuzzy C-means clustering and neural networks were used by Osareh et al. [3]. Gardner et al. proposed an automatic detection of diabetic retinopathy using an artificial neural network. The exudates are identified from grey level images by Gardner et al. [4]. In [5] a new hybrid classifier as an ensemble of Gaussian mixture model and support vector machine is proposed for exudate detection by M.U.Akram et al. As for mathematical morphology based exudate detection methods, vessels and optic disk are removed first, then mathematical morphology operators are performed to obtain the exudates. Sopharak et al.[6] used a closing operator and reconstruction operators together with thresholding to remove the optic disk and main vessels, then discriminate the exudate pixels according to the local variation due to exudate pixels have high contrast to its surrounding pixels. Retinal fundus image analysis currently attracts lots of attention from both computer science field and ophthalmology. Its aim is to develop computational tools which will assist quantification and visualization of the anatomical structures and lesions. It includes vessels analysis, optic disk analysis, macular analysis, micro-aneurysms detection and exudate detection. In this paper, we review the existing works on exudate detection since our work mainly focus on bright lesions which are exudates. Much work has been performed for exudate detection based on variety of techniques. Most techniques mentioned earlier worked on dilated pupils in which the exudates and other retinal features are clearly visible. Based on experimental work reported in previous work, good quality images with larger fields are required. The retinal images must be clear enough to show retinal detail.

2. MATERIALS AND METHOD

Digital Fundus image processing currently develop from computer science field. The method presented here can be schematically described by means of the block diagram of figure 1.

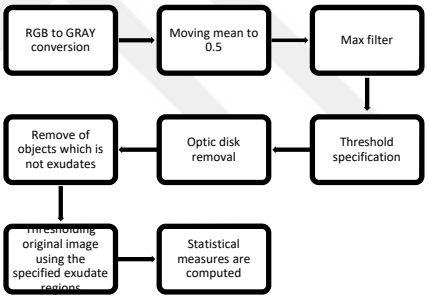

Figure 1: *Block diagram of proposed method.*

2.1. MATERIALS

In this study we tested our algorithm on forty diabetic retinopathy fundus images which have similar characteristics. These fundus images were taken from 20 females and 20 males who have exudates as a cause of Diabetic Retinopathy. They were collected from the Ankara Maya Göz Hospital. All the

results of our study have been approved by ophthalmologists Dr. Burcu Harç Kaya and Dr. Fariba Cafernejad from the Ankara Maya Göz Hospital, Turkey. All images were acquired using Topcon TRC-50EX fundus camera at 35 degree field of view. The camera were subjectively equalized for calibration, luminance and contrast before recording. The bit depth of images is 24-bit color and scaled to 1840x1224 pixels. The resolution of images are 96 dpi in horizontal and vertical dimensions. In some cases, due to the retinal surface difference, the images will have different appearance. Although some changes have been in visual features, the appearances of the fundus images were natural and bare. The method of the study was realized by using Matlab R2015b.

2.2. METHODS

In this part, the methods used are summarized; the definitions and specifications of the methods are recalled. The block diagram of the approach is provide in figure 1. In the following, we describe the steps of the algorithm.

1. RGB image is converted to gray image. Y channel of NTSC color space is computed from RGB image (equation 1). And scaled to [0,1] range. A sample fundus image converted to gray scale is given in figure 2.

$$Y = 0.2989\,R + 0.5870\;G + 0.1140\,B \quad (1)$$

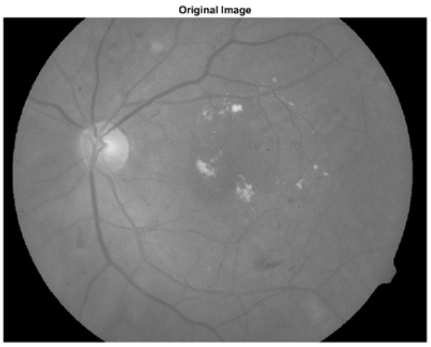

Figure 2: *A sample fundus image with exudates converted to gray scale.*

The field of view (pupil) of the fundus image is extracted. The region is specified by thresholding the image. The pixels with brightness higher than 0.1 is considered field

2. of view. If more than two connected components distinct regions are obtained by thresholding the biggest connected component (region) is regarded field of view. Next the mean brightness (value) in the field of view Y is moved to 0.5. The following linear transformation(equation 2) is employed.

$$\mathrm{I} = \frac{-1}{2\,m-2}\,Y + \frac{2\,m-1}{2\,m-2} \quad (2)$$

3. Using 21x21 size overlapping window (20 samples overlap in horizontal and vertical directions) max filter (equation 3) is applied.

$$y(m,n) = max_{i,j}\,I(n+i, m+j), i, j = -5, \dots, 5. \quad (3)$$

For the image in figure 3, the max filter output is as follows.

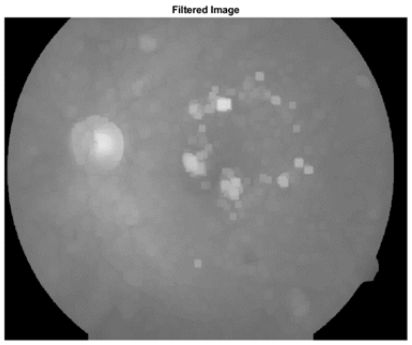

Figure 3 : *Max filter output*

4. A polygonal line consists of three line segments is fitted to cumulative histogram of image y. The cumulative histogram is given by

$$c(k) = \frac{\text{number of pixels } \leq k}{\text{total } number \text{ of pixels}}, \quad k = (0,1,\dots,255)/255. \tag{4}$$

A polygonal curve denoted by $g(k) = P(a_1, a_2, a_3, a_4; k)$ is fitted to the cumulative histogram. Here, a_n, a_{n+1} are initial and end point od n-th line segment respectively. The unknown points are optimized such that mean square of error

$e(k) = c(k) - g(k)$ is minimum:

$$\min_{a_1,a_2,a_3,a_4} \sum_{k=0}^{1} \big(c(k) - g(k)\big)^2, \quad \text{subject to } g(1) - g(0) = 1 \tag{5}$$

The polygonal curve and cumulative histogram are shown in figure 4.

The threshold is then selected as

$$\text{THR} = x(3) - 0.1\,\big(x(3) - x(2)\big) \tag{6}$$

where $x(2)$ and $x(3)$ are x- abscissa of points a_2, and a_3 respectively. The term $0.1\,\big(x(3) - x(2)\big)$ is for taking into account that slope at a_3 does not change abruptly.

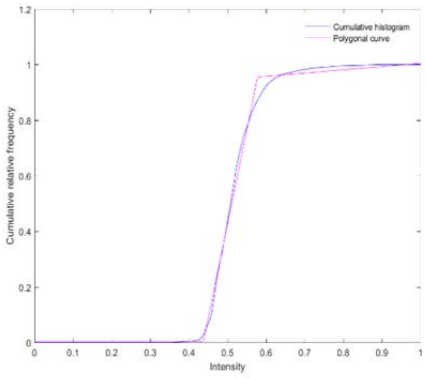

Figure 4 : *Polygonal curve and cumulative histogram*

5. After thresholding connected components are obtained and the component with highest area is considered optic disk (together with reflected light about the disk) and removed. Similarly the objects with major axis length greater than quarter of major axis length of the field of view are regarded as scattering of light from the border of the pupil.
6. To obtain final segmentation the pixels of the image I in the regions obtained are thresholded with the threshold obtained in step 4. With this threshold we detect the location of exudates which are shown in figure 5.

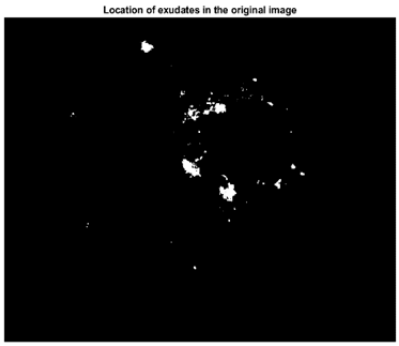

Figure 5: *Location of exudates*

7. Finally, we compute two statistical measures from the segmented image. Percentage of total exudates in the field of view = total area of exudates / pupil area. Percentage of biggest exudate = the highest exudate area / total area of exudates

3. RESULTS

In this study, we propose a simple yet an efficient method on the fundus images with dispersed exudates. In figure 6

a good segmentation of the is reported. The method removes optic disk and finds exudates.

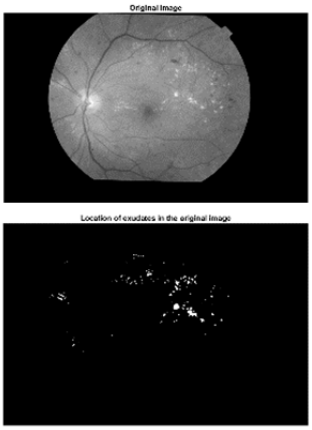

Figure 6: *Original image (left) and detected exudates (right)*

In some images, there is reflection at the boundaries of the fundus image due to camera light. This reflection effect success of exudate detection because these light reflections may be regarded exudates by the algorithm. The proposed algorithm also eliminates these reflected areas. The fundus image and its detected exudates given in figure 7 is a demonstration of this capacity.

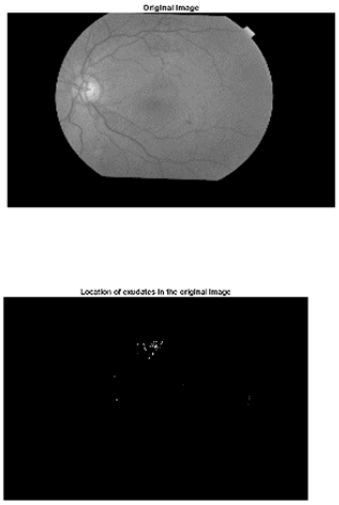

Figure 7: *Original image (left) and detected exudates (right)*

The algorithm fails when exudates are not dispersed, the groping resulted by max filter is higher than the optic disk and gives bad results when the exudates are bigger than the optic dis diameter or major axis length of the reflected light at boundaries. Figure 8 shows an example of this situation.

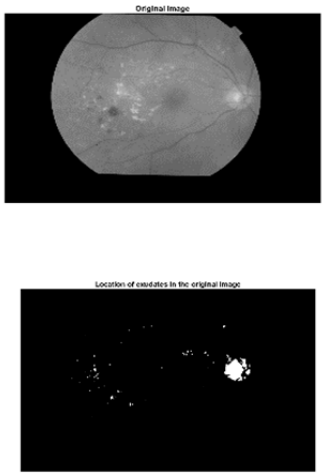

Figure 8: *Original image (left) and detected exudates (right)*

4. CONCLUSION & FUTURE WORK

With this paper, diabetic retinopathy exudates were detected. It is experimentally shown that our model performs well on the fundus images with dispersed exudates. Finally We tested the method on several color fundus images to assess the performance of our approach. We conclude that the presented method can assist ophthalmologists to specify exudates and help to overcome the problem of contrast, incorrect illumination and noise while examining the fundus images. Additionally it may also support specialist for monitoring the progression of disease and aid for a better treatment plan. Our algorithm generally perform well but when the exudates (their groping by the algorithm) are bigger than the optic disk, it cannot remove it because we do not use a disk removal technique for just removing optic disk. Simply a segmented region, after max filtering, with the biggest area is removed. We will also apply special technique for removing optic disk. Our future attempt will be detection of optic disk before the algorithm is applied for specifying exudates. Using negative of the gray image it may be possible to detect micro-aneurysms by applying this algorithms with some modifications. In addition, detection of the lesions at earlier stages is still an open problem.

5. ACKNOWLEDGEMENT

Authors would like to thank ophthalmologists Dr. Burcu Harç Kaya and Dr. Fariba Cafernejad for providing fundus images and evaluating the results of the algorithm.

6. REFERENCES

[1] K.Narasimhan, Neha.V.C, K.Vjayarekha (2012) A review of automated diabetic retinopathy diagnosis from fundus image. Journel of theoretical and applied information technology. Vol 39, pp 225-238

[2] Akara Sopharak , Bunyarit Uyyanonvara and Sarah Barman," Automatic Exudate Detection from Non-dilated Diabetic Retinopathy Retinal Images Using Fuzzy C-means Clustering" Sensors , Vol.9, pp.2148- 2161,2009.

[3] Osareh A, Mirmehdi M, Thomas B, Markham R (2003). Automated identification of diabetic retinal exudates in digital color images, British Journal of Ophthalmology, vol 87, No 10,pp 1220-1223.

[4] Gardner GG, Keating D, Williamson TH, Elliott AT(1996). Automatic detection of diabetic retinopathy using an artificial neural network: a screening tool, British journal of Ophthalmology, pp 940-944

[5] M.U.Akram, A.Tariq, S.A. Khan, M.Y.Javed(2014) Automatic detection of exudates and macula for grading of diabetic macular edema, BIOMED, pp 141-152

[6] Sopharak,A.,Uyyanonvara,B.,Barman,S. ,Williamson,T.H.,(2008) Automatic detection of diabetic retinopathy exudates from non-dilated retinal images using mathematical morphology

methods. Comput. Med. Imaging Graph. pp 720-727

[7] Dr.Prasanna Kumar, Mrs.Deepashree Devaraj, Manisha(2013) Automatic exudates detection for the diagnosis of the diabetic retinopathy, International Journal of innovative research and studies, Vol 2, pp 658-669

[8] Jayant Shah (1991) Segmentation by nonlinear diffusion, IEEE, pp 202-207

[9] T.P .Karnowski , D.Aykac, L. Giancardo , Y.Li, T.Nichols , K.W.Tobin, E.Chaum (2011) Automatic Detection of Retina Disease :Robustness to image quality and localization of anatomy structure , IEEE transactions on biomedical engineering, pp 5959-5964

[10] Yunmei Chen, B.C Wemuri, Li Wang (2000) Image Denoising and Segmentation via Nonlinear Diffusion, ELSEVIER, pp 131-149